J. agric. Engng Res. (1998) **70,** 231–256
Article Number: ag980272

REVIEW PAPER

Modelling Water Flow and Solute Transport in Heterogeneous Soils: A Review of Recent Approaches*

Jan Feyen; Diederik Jacques; Anthony Timmerman; Jan Vanderborght

Institute for Land and Water Management, Faculty of Applied Agricultural and Biological Sciences, Katholieke Universiteit Leuven, Vital Decosterstraat 102, B-3000 Leuven, Belgium

(Received 6 January 1997; accepted in revised form 15 January 1998)

A quantitative description of water flow and solute transport in the unsaturated zone of the soil is required to predict the impact of human influences on the environment. This paper starts with the basic concepts of the mathematical descriptions of transport processes in homogeneous media. However, water flow and solute transport in natural soils are significantly influenced by the occurrence of (1) macropores and structured elements (micro-heterogeneity), (2) spatial variability of soil properties (macro-heterogeneity) or (3) a combination of (1) and (2). In these cases, the classical representations of water flow and solute transport are not adequate. The paper presents an overview of some recent modelling concepts dealing with water flow and solute transport in heterogeneous media. For each model, we first introduce the underlying physical concept, and then translate the concept into a mathematical model. Each model is illustrated for a specific water flow and solute transport problem. Finally, some applications of the models are discussed. At this moment, it is difficult to specify which model should be used to solve a particular problem since no extensive validation of the models has been performed. Additional research is required to develop accurate and rapid measurement techniques for the necessary input parameters. To be useful in real environmental problems, modelling concepts for micro- and macro-heterogeneity should be coupled in one overall mathematical framework.

* Presented at AgEng 96, Madrid, Spain, 23–26 September 1996 (Opening key-note lecture of the third meeting of the EurAgEng Special Interest Group on Soil and Water chaired by Professor Daniele De Wrachien, 24 September 1996).

1. Introduction

This paper is primarily devoted to a discussion of various issues related to the modelling of water flow and the transport of solutes in the unsaturated zone. The unsaturated zone is the region through which chemicals must pass to reach the saturated zone. The various processes occurring within this region, therefore, play a major role in determining both the quality and quantity of water recharging into the saturated zone. After a brief description of the classical approach for simulating water flow and solute transport in porous media, the paper highlights some of the problems associated with the classical approach. The simplified representation of the flow (by means of the Richards') and transport (convection–dispersion, CDE) equations is not able to describe flow and transport in heterogeneous soils. Two types of soil heterogeneity which require different modelling approaches are distinguished: micro- and macro-heterogeneity. Micro-heterogeneity refers to the heterogeneity at the pore scale due to the presence of macropores which form a separate pore network and macro-heterogeneity refers to the spatial variability of macroscopic soil properties which define flow and transport at a macroscopic scale. The effect of both types of heterogeneity on water flow and solute transport is well documented in the paper. The paper also contains a comprehensive discussion of alternative modelling approaches, which make it possible to describe more accurately the flow and transport processes in heterogeneous soils, at local and field scale. They vary from the dual (multi)-porosity models, the stream tube models and the stochastic-continuum models. With respect to the stochastic approach, in the discussion, special emphasis is given to the characterization of spatial variability and the prediction of effective parameters. As heterogeneity increases, modelling approaches evolve from a purely deterministic description to a stochastic analysis.

Notation

a	fitting parameter
a	perturbation of α in Gardner equation [Eqn (22)]
a^*	characteristic length of porous media
a_r	scaling factor of scaled medium
a_w	distance from centre of a fictitious matrix block to the fracture boundary [L]
b	fitting parameter
$f_{\mathbf{Y}}$	multivariate probability density function of random variable $\mathbf{Y}$
h	perturbation of ψ
h	lag distance [L]
l^*	correlation length [L]
m	shape parameter in van Genuchten equation [Eqn (3)]
n	shape parameter in van Genuchten equation [Eqn (3)]
$\mathbf{q}$	water flux vector [L/T]
t	time [T]
v	average particle velocity [L/T]
$\mathbf{v}$	velocity vector [L/T]
w_i	weighting factor of *i*th subsystem in multi-model porosity models
$\mathbf{x}$	vector with spatial coordinates
y	perturbation of $\ln K_s$
$\mathbf{y}$	vector with realizations of random variables
z	depth [L]
$z(\mathbf{x})$	realization of random space function
A	expected value of α in Gardner equation [Eqn (22)]
C	solute concentration [M/L^3]
C_0	concentration of leaching solution [M/L^3]
$\mathbf{D}$	dispersion tensor [L^2/T]
D_{eff}	effective dispersion [L^2/T]
E	spatial domain $\subset \mathbb{R}^3$
$E[\cdot]$	expectation operator
H	mean pressure head (expected value of ψ)
$\mathbf{I}$	unity matrix
$\mathbf{K}$	conductivity tensor [L/T]
K_a	conductivity of exchange term in dual-porosity model [L/T]
K_{eff}	effective hydraulic conductivity [L/T]
K_r	relative hydraulic conductivity
K_s	saturated hydraulic conductivity [L/T]
$K^*(\theta)$	reference hydraulic conductivity
N	number of subsystems in multi-modal porosity models
S_e	effective saturation
S_{ei}	effective saturation of *i*th subsystem in multi-model porosity models
S_{hh}	spectrum of h fluctuations
T	output variable of a simulation model
Var	time variance of a solute breakthrough curve [T^2]
Y	expected value of $\ln K_s$
$\mathbf{Y}$	vector of random variables
$Z(\mathbf{x})$	random space function
α	shape parameter in van Genuchten equation [Eqn (3)] [L^{-1}]
α	parameter in Gardner equation [Eqn (22)] [L^{-1}]
α_s	first-order diffusive transfer coefficient [T^{-1}]
α_w	first-order advective transfer coefficient [L/T]
β	shape factor in dual porosity model
γ_w	empirical coefficient in dual-porosity model
δ_{ij}	Kronecker delta
$\varepsilon(\mathbf{x})$	stochastic variability of a Random Space Function [RSF]
θ	volumetric water content [L^3/L^3]
θ_i	volumetric water content in pore region i (dual-porosity models)
θ_r	residual water content
θ_s	saturated water content
λ_L	longitudinal dispersivity [L]
λ_T	transverse dispersivity [L]
$\mu(\mathbf{x})$	deterministic variability of a RSF
ξ	coordinates of travel path of solute particle
ρ_{vivj}	the spatial (cross) correlogram between the *i*th and *j*th component of the velocity vector
σ^2_{Xij}	The *ij*th entry of Σ_X
σ^2_{vivj}	the *ij*th entry of the velocity covariance matrix
τ	tortuosity factor
ψ	pressure head [L]
$\psi^*(\theta)$	reference pressure head [L]
ψ_f	pressure head in macropore domain [L]
ψ_m	pressure head in matrix domain [L]
Γ_s	solute interaction term (dual-porosity models) [M/T]
Γ_w	water interaction term (dual-porosity models) [1/T]
Σ_X	covariance matrix of the particle locations
Φ	hydraulic head [L]

2. Classical approach to model water flow and solute transport in porous media

2.1. *Water flow*

To describe water flow processes in a porous medium, the continuum approach is used to derive the water flow equations. The properties of the porous medium as well as the dynamic and kinematic variables of the fluid are averaged over a representative elementary volume, REV.[1] The REV must be large enough so that the averages, when assigned to the centroid of the REV, are continuous functions in space, but small enough so that macroscopic properties or variables relevant for the description of the flow process are obtained. Since the macroscopic variables and properties are continuous functions in space, differentials are defined and partial differential equations based on mass, momentum and energy conservation can be used to describe water flow in a porous medium.

Assuming laminar flow and neglecting the inertial terms of the momentum conservation equation, the macroscopic water flux is linearly related to the hydraulic head gradient and the Darcy flow equation is obtained:

$$\mathbf{q} = -\mathbf{K}\cdot\nabla(\Phi) \tag{1}$$

where $\mathbf{q}$ is the water flux vector, $\mathbf{K}$ the conductivity tensor and Φ the hydraulic head. In rigid unsaturated soils, the hydraulic head consists of the elevation head, z, and the pressure head, ψ, which results from capillary forces and is negative. Based on mass conservation, the Richards' flow equation is obtained:[2]

$$\frac{\partial\theta(\psi)}{\partial t} = \nabla\cdot(\mathbf{K}(\psi)\nabla(\psi + z)) \tag{2}$$

where θ is the volumetric water content. The water retention characteristic, $\theta(\psi)$, and the conductivity characteristic, $\mathbf{K}(\psi)$, are soil (layer)-dependent hydraulic properties that have to be determined in order to model water flow by means of the Richards' equation. These characteristics can be determined from direct measurements of both θ and ψ, and $\mathbf{K}$ and ψ. Alternatively, using inverse optimization techniques, $\theta(\psi)$ and $\mathbf{K}(\psi)$ characteristics can be found by fitting the solution of the Richards' flow equation to observed variables ($\mathbf{q}, \theta$ or ψ) in controlled flow experiments.

One of the most popular analytical functions for $\theta(\psi)$ is the one proposed by van Genuchten[3] and is given as

$$S_e = \frac{1}{(1 + (\alpha\psi)^n)^m} \tag{3}$$

where $S_e = (\theta - \theta_r)/(\theta_s - \theta_r)$ is the effective saturation, θ_s and θ_r are the saturated and residual water content, respectively, and α, n and m are shape parameters. If $m = 1 - 1/n$, then the hydraulic conductivity model of Mualem[4] can be written in terms of the parameters of Eqn. (3). The relative hydraulic conductivity, $K_r(\psi) = K(\psi)/K_s$ with K_s the saturated hydraulic conductivity, becomes

$$K_r(\psi) = \frac{(1 - (\alpha\psi)^{n-1}(1 + (\alpha\psi)^n)^m)^2}{(1 + (\alpha\psi)^n)^{m\tau}} \tag{4}$$

with the same parameters as described above and τ, a parameter describing the tortuosity (mostly choosen as 0·5[4]). *Figure 1a* shows the water retention characteristic together with its first derivative, the pore-size distribution, of a homogeneous sandy loam soil. The pore-size distribution expresses the fraction of pore space that drains at a given pressure head. *Figure 1b* shows the unsaturated hydraulic conductivity for the same soil. These properties will be used to model water flow and solute transport in a homogeneous soil profile. Examples are given in *Figs 1c* and *d* and will be discussed below. Combinations of the retention curve with other conductivity models such as those of Gardner,[5] Gilham *et al.*[6] and Brooks and Corey[7] can be used as well.

To model the field-scale water balance, the one-dimensional formulation of the Richards' equation, assuming horizontally uniform soil layers and predominantly vertical water flow, is solved numerically by various computer codes, e.g. WAVE.[8] *Figure 1c* shows the infiltration of water into a soil profile after 0·1 d with the following initial and boundary conditions:

$$\psi = -500\,\text{cm}, \quad 0 < z < -100\,\text{cm} \quad \text{at } t = 0 \tag{5a}$$

$$\psi = 0\,\text{cm}, \quad z = 0\,\text{cm} \quad \text{at } t > 0 \tag{5b}$$

$$q = -K(\psi), \quad z = -100\,\text{cm} \quad \text{at } t > 0 \tag{5c}$$

where z is the depth coordinate. The hydraulic properties of this soil are shown in *Figs 1* and *b*. The top 18 cm is saturated with water after 0·1 d of ponding (*Fig. 1c*) and a small transition zone, where the water content is larger than the initial water content but smaller than the saturated water content, is observed between a depth of 18–30 cm.

2.2. *Solute transport*

The transport of solutes into a porous medium is quantified by two variables, i.e. (1) the average solute particle velocity, and (2) the solute dispersion. The average solute particle velocity defines the centroid of the solute plume at a given time or the average arrival time of solutes at a given depth. For a homogeneous porous medium, steady-state water flow and an inert solute, the

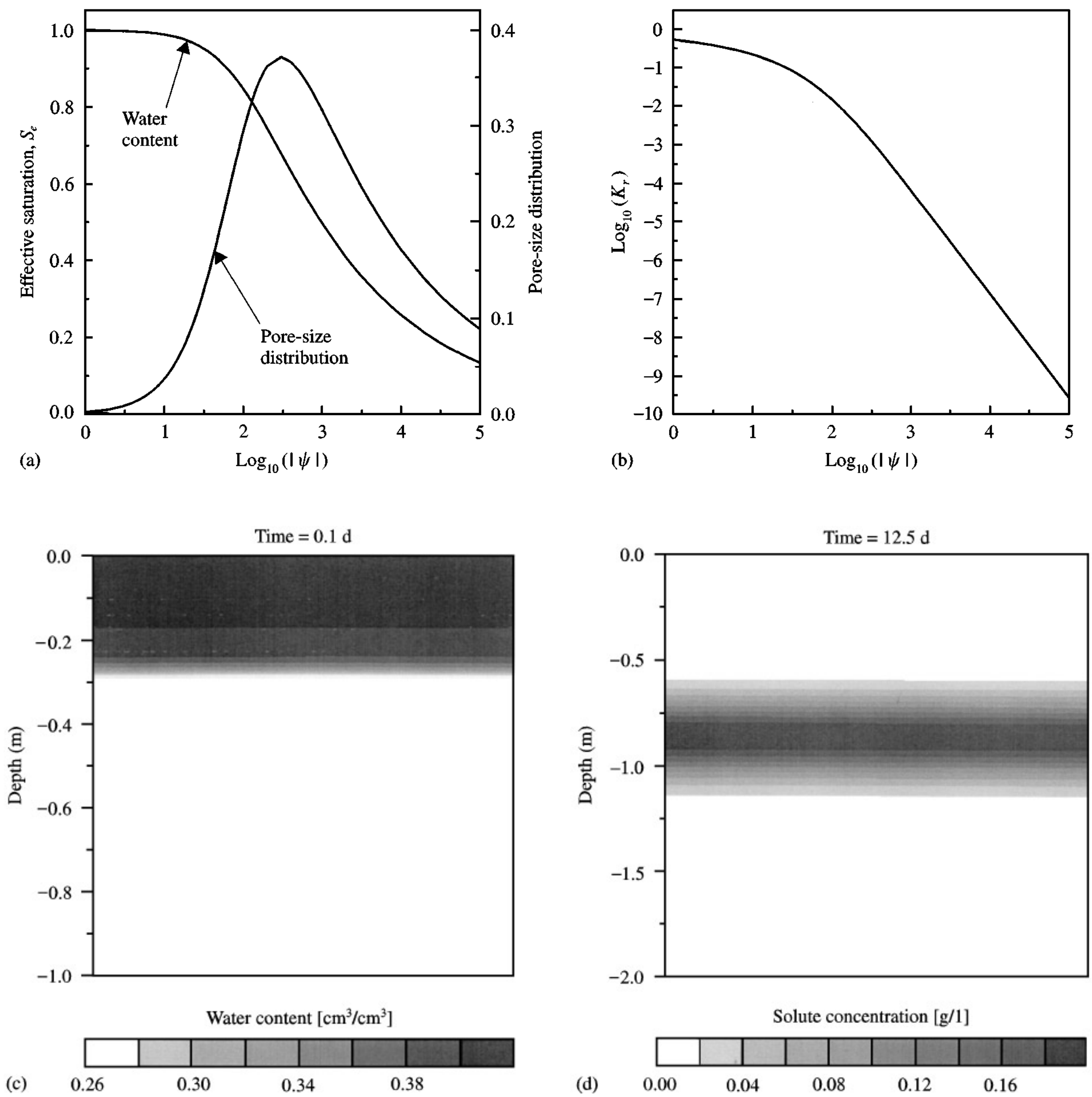

Fig. 1. Hydraulic properties of a homogeneous soil: (a) $\theta(\psi)$ and pore-size distribution with $\alpha = 0{\cdot}0109\,cm^{-1}$ and $n = 1{\cdot}288$; (b) $K_r(\psi)$ for parameters given in (a) and $\tau = 0{\cdot}5$; (c) water content profile after time 0·1 d for boundary and initial conditions given by Eqns (5a)–(5c) using WAVE;[8] (d) solute distribution at time 12·5 d after solute application under steady-state flow conditions ($q = 2{\cdot}8$ cm/d) for boundary and initial conditions given by Eqns (8a)–(8c) using WAVE[8]

average solute particle velocity equals $\mathbf{q}/\theta$. The solute dispersion quantifies the dispersion of the solute plume around the centroid at a certain time or the dispersion of the solute breakthrough around the average arrival time at a certain depth. In porous media, solute dispersion is caused by two mechanisms: (1) molecular diffusion and (2) hydrodynamic dispersion. Hydrodynamic dispersion is explained by the tortuous nature of the convective stream lines resulting from microscopic fluctuations of the advection velocity. When the scale of the macroscopic transport process is much larger than the scale of the microscopic velocity fluctuations, the effect of these fluctuations on the macroscopic solute transport can be modelled as a Fickian, gradient-type process, similar to molecular diffusion.[9] Using the continuum approach, the macroscopic solute mass conservation equation is, for non-adsorbing and non-degradable solutes, written as

$$\theta\frac{\partial C}{\partial t} + \theta\mathbf{v}\cdot\nabla C - \nabla\cdot(\theta\mathbf{D}\cdot\nabla C) = 0 \qquad (6)$$

where C is the solute concentration, $\mathbf{v}(=\mathbf{q}/\theta)$ the velocity vector, and $\mathbf{D}$ the dispersion tensor. Equation (6) is the general form of the convection–dispersion equation. According to Bear,[1] the dispersion tensor is defined as

$$D_{ij} = \lambda_T |\mathbf{v}| \delta_{ij} + (\lambda_L - \lambda_T) \frac{\mathbf{v}_i \mathbf{v}_j}{|\mathbf{v}|} + \tau(\theta) D_m \delta_{ij} \tag{7}$$

where λ_L and λ_T are the longitudinal and transverse dispersivity, δ_{ij} the Kronecker delta, $\tau(\theta)$ the tortuosity factor which depends on the water content[10] and D_m the molecular diffusion coefficient. λ_L, λ_T and $\tau(\theta)$ are soil-specific parameters that have to be determined experimentally from tracer experiments.

As an example, solute movement under a steady-state water flux of 2·8 cm/d was modelled. The initial and boundary conditions for the solute transport problem are

$$C = 0, \quad 0 < z < -200\,\text{cm} \quad \text{at } t = 0 \tag{8a}$$

$$C - \frac{D}{v}\frac{\partial C}{\partial z} = 50\,\text{g/l} \quad \text{at } 0 < t < 0{\cdot}02\,\text{d} \tag{8b}$$

$$C - \frac{D}{v}\frac{\partial C}{\partial z} = 0\,\text{g/l} \quad \text{at } t > 0{\cdot}02\,\text{d} \tag{8c}$$

In *Fig. 1d*, the concentration profile is shown at 12·5 d after solute application for a soil having the hydraulic properties displayed in *Figs 1a* and *b*, and a dispersivity of $\lambda_L = 1$ cm. For one-dimensional transport, Eqn (7) simplifies to a linear relation between D and v:

$$D = \lambda_L v + \tau(\theta) D_m \tag{9}$$

This linear relation was evident from various leaching experiments under saturated conditions in repacked sands.[11] Using an interacting flow region model, Skopp and Gardner[12] demonstrated that the linear relation between D and v is valid only if (1) the variance of the microscopic velocity fluctuations relative to the average pore water velocity does not change with increasing flow rate and (2) the mixing of solutes between zones with different velocities is proportional to the flow rate which means that mixing occurs due to horizontal advection of solutes. Although the linear relation between D and v is always used for modelling solute transport under transient conditions in unsaturated soils, leaching experiments in unsaturated highly structured soils revealed that λ_T increased drastically with increasing flow rate.[13,14]

3. Problems with the classical approach to model water flow and solute transport in heterogeneous soils

3.1. *Micro-heterogeneity due to macropores and soil structure*

Before illustrating the effect of macropores on water and solute transport, it is important to mention that an unequivocal definition of macroporosity does not exist, in part because there are several forming processes resulting in macropores of different size, shape and continuity, and in part because the soil material (texture) has an impact (what can be seen as macropores in a fine textured clay soil, can just be a part of the bulk soil volume in a coarse textured sandy soil). A detailed discussion on the types of macropores and their hydrodynamic behaviour is however beyond the scope of this article, but can be found in Refs 15–17. A theoretical but workable definition, amongst many other definitions, could be the following: “macropores are that part of the soil volume, except stones and biological species, constituting an obvious deviation from the normal packing of primary soil particles and, consequentely, water flow and solute transport processes cannot be described with the classical approach”.

3.1.1. *Illustration of the effect of macropores and soil structure on water flow*

In the absence of a continuous macropore network, water flow in a homogeneous, non-macroporous soil obeys the classical water flow theory based on the Buckingham–Darcy law. However, when macropores are present this theory may not adequately describe the infiltration and redistribution of water as shown by Mallants *et al.*[18] Although these macropores may comprise only a small fraction of the total soil volume, they can have a profound effect on the rate of infiltration and redistribution of water under certain conditions depending on the amount of water supply to the soil surface, the initial moisture content of the soil matrix and the microrelief of the surface. This behaviour is described several times in literature as “channelling flow”, “preferential flow”, “short-circuiting” or “bypass flow” (Refs 19–21, 15 and 16 amongst many others).

A clear example showing the impact of macropores on water flow is presented in *Fig. 2* which displays the results of a field experiment Nine time-domain reflectometry probes (TDR probes) were installed under the soil surface (*Fig. 2a*) in a grid of 3×3 to measure local moisture contents (*Fig. 2b*). Three different doses of a 0·1% concentrated methylene blue (MB) dye solution[22] and one dose of a 0·5% concentrated acid red I (ARI) dye solution[23] were uniformly applied to the soil surface as four dirac input pulse functions during the experiment (*Fig. 2b*).[24] After the infiltration of the dye solutions, the soil was sectioned at seven depths to visualize staining patterns indicating preferential flow paths of water. (*Figure 2c* shows three horizontal sections at the insertion depths of the TDR probes, i.e. at a depth of 25, 41 and 55 cm.) It is clear from *Fig. 2b* that the TDR probes 3, 6 and 9 show a profound increase of moisture content indicating macropore flow through surface-vented and continuous macropores. This is in agreement with *Fig. 2c*

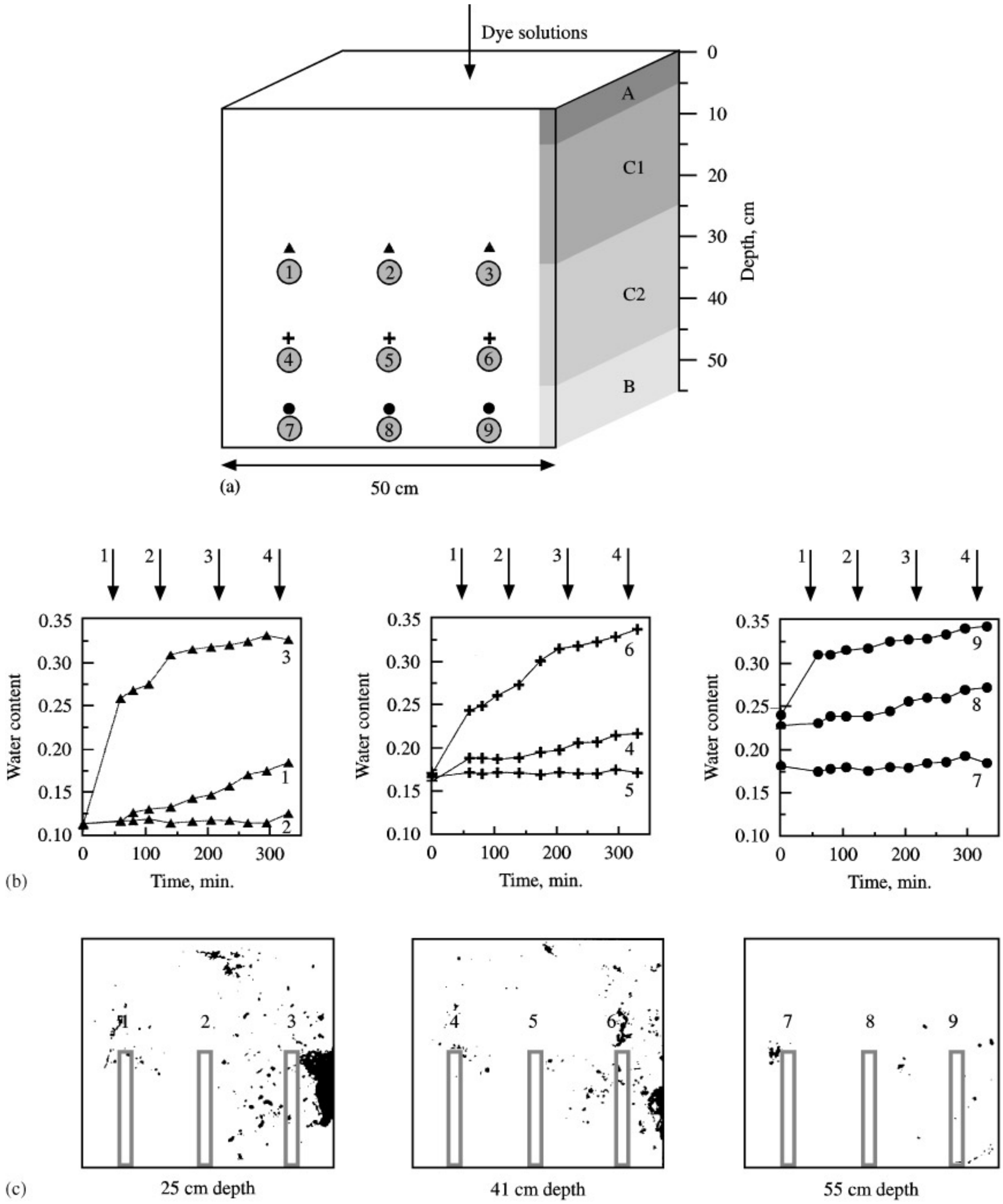

Fig. 2. Experimental arrangement (a) and results (b and c) from an infiltration experiment with dye solutions in the field. (b) shows the increase in water content detected by the TDR probes after application of a series of dye solutions in four steps (1 = 10 mm of MB, 2 = 15 mm of MB*, 3 = 20 mm of MB* and 4 = 30 mm ARI**) and (c) displays the horizontal staining patterns of methylene blue at the insertion depth of these probes, together with the measurement area of these probes (open bars). * MB = 0·1 % concentrated methylene blue dye solution; ARI** = 0·5 % concentrated acid red I dye solution*

where it can be seen that most of the staining patterns (especially at the first two insertion depths) are present around these probes. The increase of moisture content detected by TDR probe 8 indicates redistribution of water from macropores to the matrix, when these macropores end at greater depth in the profile (also called "internal catchment" by Bouma[17]), since the TDR probes located above TDR probe 8 (2 and 5) detect no or only a small increase of moisture content. This is in agreement with the location of a large red-staining pattern on the right-hand side bottom corner of the field plot at 55 cm depth (not shown here).

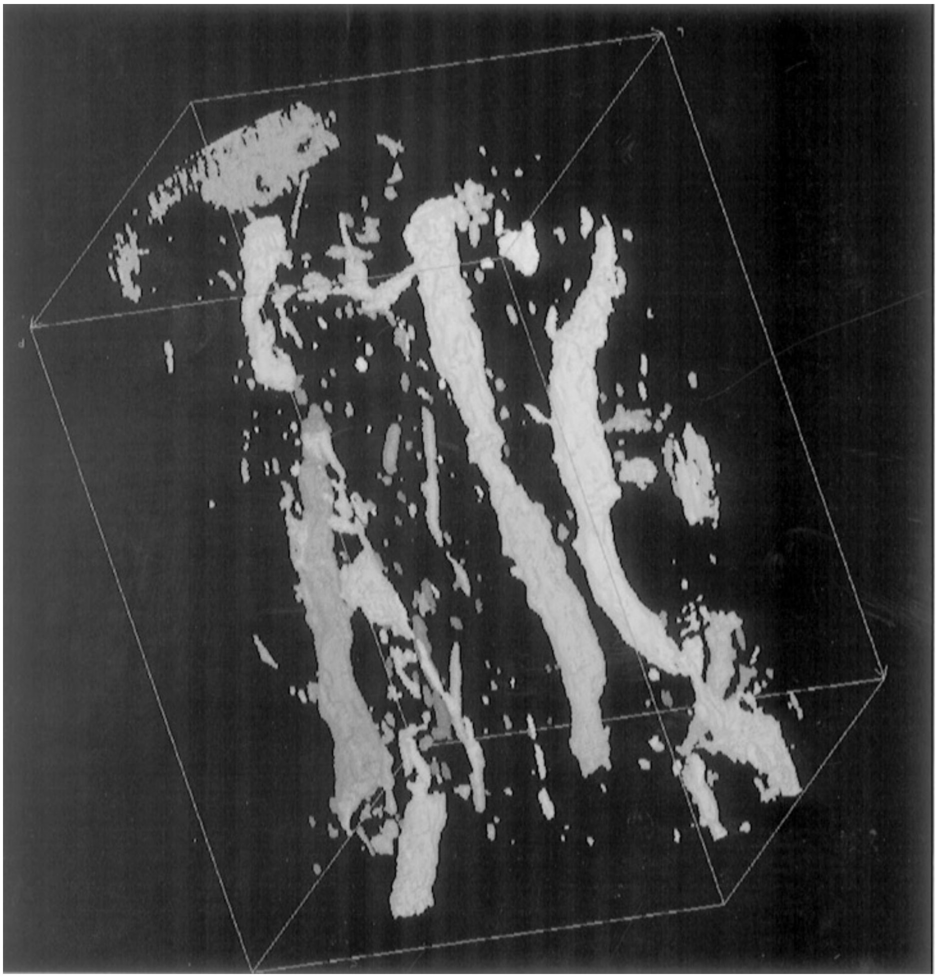

Fig. 3. Three-dimensional surface rendered image of a macropore network after scanning a 15 cm long, 10 cm internal diameter soil core with a medical CT scanner[25]

Another example clearly showing the influence of macropores on water flow is presented in *Fig. 3*. This figure shows a three-dimensional surface-rendered macropore network (with a continuous macropore from top to bottom) achieved from scanning a soil core (10 cm i.d., 15 cm long) with a medical CT scanner and a depth increment of 1 mm.[25] This kind of information, which can hardly be achieved from dye or impregnation experiments, enables us to explain the very high saturated conductivity (478 cm/d) measured on this soil core. Moreover, this kind of data should provide additional information for input (structure parameters) in existing water and solute transport models.

3.1.2. *Illustration of the effect of macropores and soil structure on solute transport*

The effect of macropores on solute transport can be illustrated by solute breakthrough curves.[16,17] Relative solute concentrations, C/C_0 with C_0 the concentration of the leaching solution, which was measured in the effluent during steady-state and transient flow leaching experiments in a 1 m long undisturbed macroporous loam soil column are shown[26] in *Figs 4* and *5*. For the transient flow leaching experiment, a certain amount of solution with concentration C_0 (8·3 cm infiltration depth) was added daily over a small time period (3 h), whereas for the steady-state flow experiment, the same amount of solution was applied daily, but a constant flow rate was maintained at the top of the soil column. The relative concentrations shown for the transient leaching experiment in *Fig. 4* represent concentrations measured in the effluent which was collected over a 1 d period, whereas relative concentrations measured in the effluent which was collected over a shorter time period are shown in *Fig. 5*. Since the flow rate during the solute application was much higher, by a factor of eight, for the transient than for steady-state flow leaching experiments, flow and transport through macropores occurred during the transient flow experiment, whereas flow occurred mainly through the matrix during the steady-state experiment.

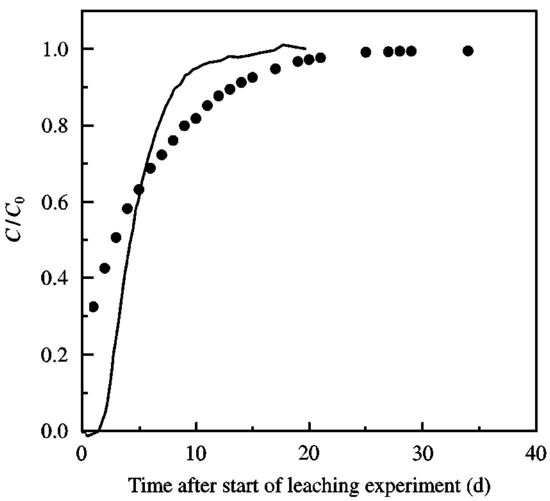

Fig. 4. Outflow solute concentrations for steady-state and non-steady-state flow conditions from a 1 m long undisturbed soil column. Solute concentration for the non-steady-state flow experiment was measured in the effluent that was collected over a 1 d period (period of the solute application): • *transient flow, macropores activated;* —— *steady-state flow, macropores not activated*

These figures clearly demonstrate how macropore flow influences solute transport and results in a different solute transport behaviour than the classical convective–dispersive transport. A typical breakthrough curve (BTC) when macropore flow occurs, is characterized by a rapid increase of solute concentration and a long tailing (*Fig. 4*). When the solution of the convection–dispersion equation is fitted to such breakthrough curves, the fitted average particle velocity, v, is higher than q/θ, the expected average particle velocity for the case of piston flow.[27,28] This higher particle velocity is explained by solutes that are convected in macropores and "bypass" the soil water in the matrix. Bypass flow depends largely on the flow rate since macropores are only "activated" when the inflow rate exceeds the infiltration rate of the soil matrix. Therefore, the water application regime may largely influence the amount of "bypass" flow in structured soils which tends to be larger for intermittent than for continuous water application.[29]

Another important characteristic of solute transport processes in structured soils is the large increase of solute dispersion with increasing flow rate since more macropores are activated and the variability of the solute particle velocity increases drastically (*Fig. 4*). As a consequence, the linear relation between v and D is not applicable for structured soils. The following relation between v and D was found to be more appropriate:[30]

$$D = av^b \qquad (10)$$

with $b > 1$, and a, b being fitting parameters.

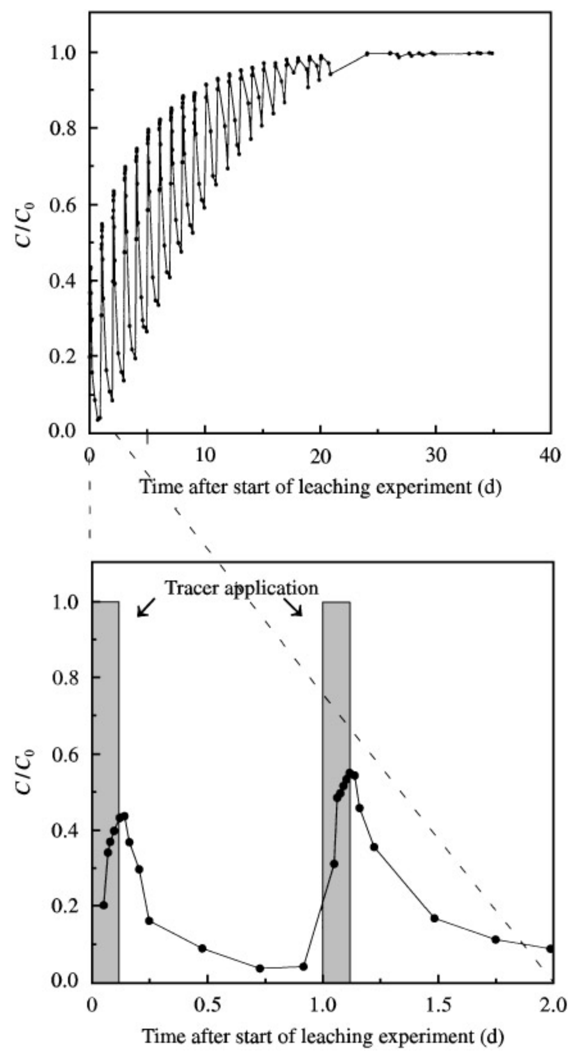

Fig. 5. Outflow solute concentrations for non-steady-state flow condition from a 1 m long undisturbed soil column. Solute concentrations were measured in the effluent collected over smaller time periods than the time period of the solute application. The lower figure is an enlargement of the upper figure over a period of 2 d

Finally, the lack of mixing of fast moving solutes (in the macropores) with slowly moving solutes (in the soil matrix) results in an apparent increase of D with depth when D is fitted to BTCs observed at different depths in the soil profile.[14] This lack of mixing is also evident from the non-monotonic behaviour of the outflow solute concentrations during the non-steady flow leaching experiment (*Fig. 5*). The decrease of effluent concentration after the tracer application stopped, indicates that macropore and matrix solution did not mix completely. At the end of an infiltration drainage cycle, when the macropores drained nearly completely, the concentration in the effluent represents mainly the concentration of the solution in the soil matrix. If the solutions in the macropore and matrix regions did mix completely, the concentration in the effluent at the end of the infiltration drainage cycle would be equal to the effluent concentration at the times when macropore flow occurs.

Since the classical CDE equation and the linear relation between D and the flow rate, v, do not account for (1) "bypass" flow and incomplete mixing of macropore and matrix soil solution and (2) the large increase of solute dispersion with increasing flow rate and depth in macroporous soils, solutes may reach a certain depth much faster than that predicted by the classical CDE equation.

3.2. *Macro-heterogeneity due to spatial variability of macroscopic soil properties*

One of the main applications of physically based water flow and solute transport models is the simulation of field-scale solute transport in the unsaturated zone. In general, the parameters necessary to solve the transport equations are determined in the laboratory, the so-called local-scale parameters. If no macropores are present, the Richards' equation and the CDE can be applied to model flow and transport at the measurement scale. However, extrapolating these local-scale parameters to predict field-scale-related problems is difficult due to the spatial and temporal variability of macroscopic soil properties which determine the local-scale parameters.

Field-scale tracer experiments have demonstrated that water and solute flow paths and distribution patterns are extremely complex and irregular in a soil profile, such as horizontal redistribution of solutes,[31] preferential movement through macropores[32] or fingered flow,[33] amongst others. *Figure 6* illustrates the water distribution after 0·5 d drainage of an initially saturated macroporous sandy-loam soil at Bekkevoort, Belgium. In the same soil, local solute concentrations were measured using horizontally installed TDR probes at five depths and at 24 locations at each depth.[34] Four BTCs at each depth are shown in *Fig. 7* to illustrate the spatial variability of solute transport, using Cl^- as a tracer.

Near the soil surface, most variability is found in different peak concentrations, whereas deeper in the soil, BTCs differ in both the arrival time of the peak concentration and the solute dispersion.

The variability of transport processes is caused by the spatial variation of soil properties in natural fields (e.g. see Ref. 35 for a review). A clear indication of the variability are the distinct soil layers in a soil profile which may have different transport properties, e.g. hydraulic properties[36–38] with depth. The effect of soil layering on solute transport was experimentally demonstrated by Ellsworth *et al.*,[39] van Weesenbeeck and Kachanoski[40] and Feyen *et al.*[41] Large-scale variation in the horizontal direction,

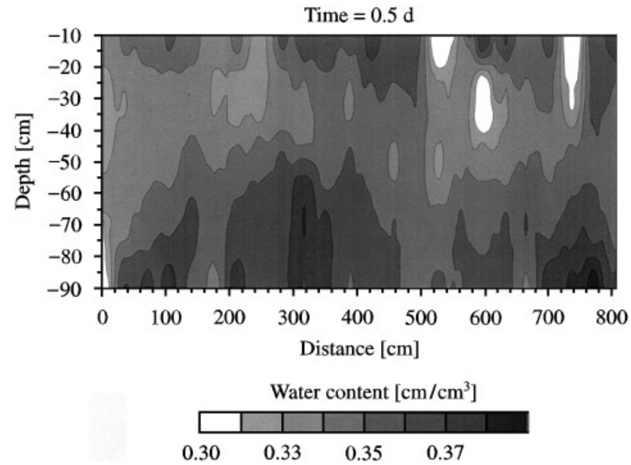

Fig. 6. Water content distribution during an in situ drainage experiment in an initially saturated sandy-loam macroporous soil after 0·5 d

e.g. two distinct soil types within a single field or a trend along a slope, also exists. This kind of variation will be referred to as deterministic large-scale variability.

Soil properties exhibit, in addition to the deterministic, also stochastic small-scale variability around the mean behaviour of the properties in all directions. This small-scale variability is widely recognized, especially for the hydraulic properties (e.g. Refs 42–45). It is shown in theoretical studies that the heterogeneity of the hydraulic properties affects the transport processes at the field scale.[46–49]

Both the deterministic and the stochastic variability of soil properties cause the scale dependency of transport parameters. This means that transport parameters are dependent on the scale or volume over which transport processes – water flow or solute transport – are averaged. A typical example of the scale dependency is the increase in the dispersion coefficient for increasing volumes of averaging BTCs. This can be explained in the following way. Local-scale BTCs may differ significantly in their shape, as shown in *Fig. 7*. Averaging these local-scale BTCs results in mean BTCs with an enlarged spread compared with the spreading in the local BTCs. This is illustrated in *Fig. 8* using the approach of van Weesenbeeck and Kachanosiki[50] for a loamy soil. At a depth of 90 cm local-scale BTCs were measured at 24 locations. The spatial scale (X-axis) indicates the distance over which local-scale BTCs are averaged, e.g. all local BTCs located within a distance of 4 m are averaged and the obtained averaged BTC corresponds with the spatial scale of 4 m. The spreading of the averaged BTC is expressed as the time variance of the BTC, Var $[T^2]$. Since several averaged BTCs are available at most spatial scales, the average of the time variances, $E[\mathrm{var}]$, is given on the Y-axis. The spreading of the BTC increases sharply between spatial scales of 0 and 1·5 m and 3 and

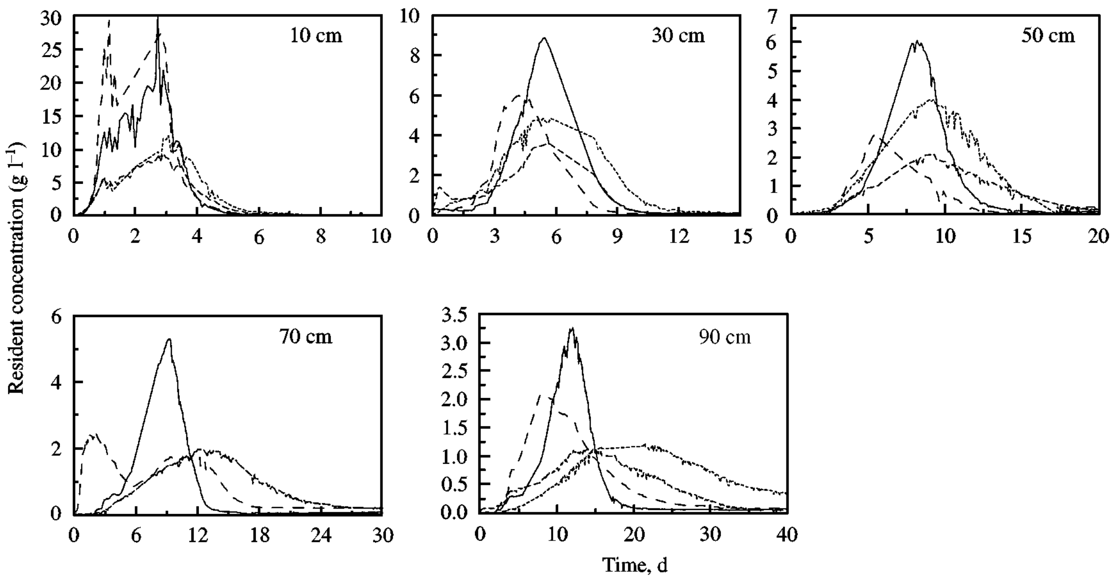

Fig. 7. Variability of solute BTCs of Cl^- at five different depths as measured during steady-state water flow ($q = 2{\cdot}8$ cm d) in aoamy macroporous soil: —— maximum concentration; – – – – – minimum concentration; - - - - - - earliest arrival; . . . . latest arrival

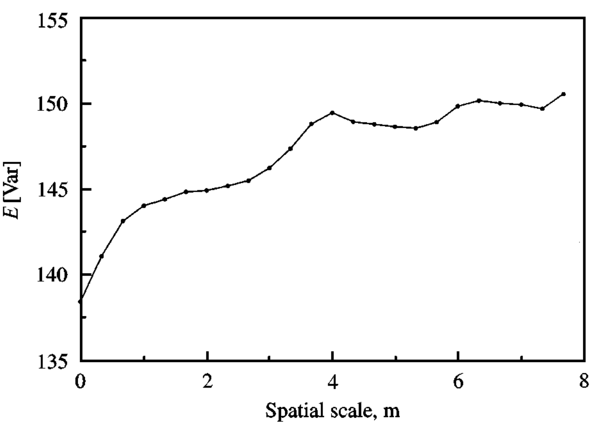

Fig. 8. Solute travel time variances E[Var], as a function of spatial scale of in situ steady-state conservative solute transport in a loamy macroporous soil

4·5 m. Thus, the solute spreading is increased due to the local-scale variability in solute breakthrough (between 0 and 1·5 m). The smooth and relatively negligible increase beween 1·5 and 3 m indicates that most of the local-scale variability is captured within approximately 2 m. However, a second significant increase in solute spreading is observed if the scale is extended. This may indicate a shift in local-scale soil properties at a spatial scale of 3 m and larger.

4. Alternative modelling approaches

In the remainder of the paper, we describe models dealing with either micro- or macro-heterogeneity. The modelling concept for each type of heterogeneity will be introduced and defined in mathematical formulations. To illustrate the idea of the model concept, the necessary input parameters are shown in an equivalent way as those required for the classical approach (*Figs 1a* and *b*). Subsequently, water flow and solute transport simulations for the initial and boundary conditions defined in Eqns (5a)–(5c) and (8a)–(8c), respectively, using the alternative approaches are compared with the simulations of the classical approach (*Figs 1c* and *d*). Finally, we discuss some applications and performance of the models using laboratory and field data.

4.1. *Dual-porosity models for "micro-heterogeneous soils"*

The Richards' equation is commonly used to describe water flow in homogeneous soils. However, when macropores are present, the one-domain approach is no longer a reliable modelling approach because two flow types can occur in one medium. Therefore, the two-domain concept or double-, dual-, bi (multi) modal-porosity models, with macropores as a second domain next to the less permeable micropore region, are nowadays widely accepted for modelling water flow and solute transport in micro-heterogeneous soils. Both regions are treated as continua, and the continuum approach is used to establish the flow and transport equations in each region. The equations for the separate pore regions are coupled by means of an exchange term accounting for the mass transfer of water and solutes between both regions.

4.1.1. *Dual-porosity models for water flow*

When the soil is (nearly) saturated, vertical water flow will be dominated by the flow in the macropores. These pores drain at low suctions so that a rapid decline of moisture content and especially of hydraulic conductivity occurs with only small suction increments near saturation (*Figs 9a* and *b*). Therefore, it is difficult to obtain detailed data of hydraulic conductivity near saturation.

Some techniques providing data on the $K(\psi)$ relationship near saturation (e.g. infiltrometers[51] and crust

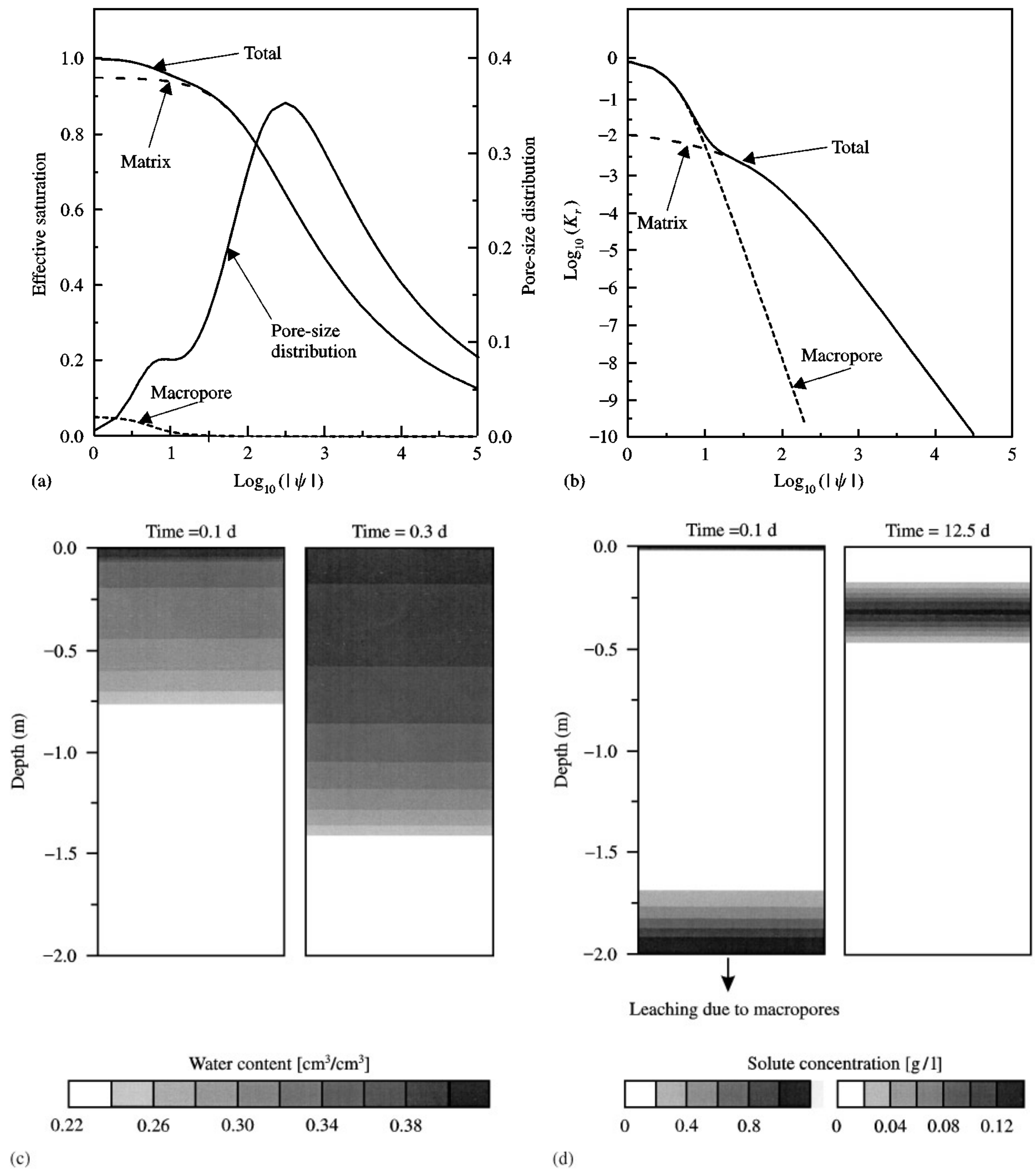

Fig. 9. Hydraulic properties of a heterogeneous, macroporous soil (a) bimodal $\theta(\psi)$ and pore-size distribution with $w_1 = 0{\cdot}05$, $\alpha_1 = 0{\cdot}2\ cm^{-1}$, $n_1 = 2{\cdot}5$, $w_2 = 0{\cdot}95$, $\alpha_2 = 0{\cdot}0109\ m^{-1}$ and $n_2 = 1{\cdot}288$; (b) bimodal $K_r(\psi)$ for parameters given in (a), $\tau = 0{\cdot}5$, $K_{s,1} = 981$ cm/d, $K_{s,2} = 1$ cm/d and $K_{s,exchange} = 0{\cdot}01$ cm/d (with subscript 1 = macropore domain and subscript 2 = matrix domain); (c) water content profile after 0·1 and 0·3 d for boundary and initial conditions given by Eqns (5a)–(5c) using DUALP_1D[61]; (d) solute distribution at 0·1 and 12·5 d after solute application under steady-state flow conditions ($q = 2{\cdot}8$ cm/d) for boundary and initial conditions given by Eqns (8a)–(8c) using DUALP_1D[61]

method[52]) have some major drawbacks. Most of these techniques are labour-intensive and measurements can only be done over a small range of pressure heads ($0 < \psi < -30$ cm). Therefore, the use of indirect methods where $K(\psi)$ or $K(\theta)$ is estimated from more easily measured soil properties, such as the moisture retention curve (and the derived pore-size distribution), has become more and more common.[53]

However, to obtain absolute conductivity values, the conductivity curve must be scaled with a "matching" value. According to van Genuchten and Nielsen,[54] Mualem[55] and Nielsen and Luckner,[56] it is advisable to take another point rather than the saturated hydraulic conductivity as a matching point because the large pores which have only slight relation to the rest of the pore-size distribution, govern the shape of the conductivity curve close to saturation (*Fig. 9b*). If an unsaturated hydraulic conductivity value is used as a matching factor, the estimates of conductivity near saturation may be largely underestimated by Mualem's conductivity model when macropores are present.

This problem arises because (1) the unimodal van Genuchten[3] retention curve is not flexible enough to describe $\theta(\psi)$ data near saturation when macropores are present and (2) the Mualem conductivity model postulates that pores with a specific size or diameter are randomly connected with other pores. The latter assumption is clearly not met when larger pores form an independent macropore network. Therefore, a new approach has been introduced to fit the retention curve by double- or bi-modal-porosity models, which are constructed by a linear superposition of subcurves of the van Genuchten[3] type:[57–59]

$$S_e = \sum_1^N w_i \left[\frac{1}{1 + (\alpha_i \psi)^{n_i}} \right]^{m_i} \tag{11}$$

where S_e is the effective saturation of the total system, N the number of subsystems that form the total pore-size distribution (indicated by "macropore" and "matrix" in *Fig. 9a*), w_i a weighting factor ($\sum w_i = 1$) and α_i, n_i and m_i the shape parameters for each subsystem [see Eqn (3)].

Due to the increased number of coefficients, the model is able to fit more accurately the $\theta(\psi)$ data near saturation. When the pore system is however not distinctly bimodal, the parameters of these curves cannot be considered as having a physical meaning but are rather shape coefficients.[59,60] The relative hydraulic conductivity function is computed based on the multi-modal representation of the retention function:

$$K_r = \sum_1^N w_i K_{ri} \tag{12}$$

with K_{ri} derived from $[1/(1 + (\alpha_i \psi)^{n_i})]^{m_i}$ by the Mualem model equation (Eqn (4); see *Figs 9a* and *b*].

Gerke and van Genuchten[61] developed an one-dimensional simulation model which describes water flow in both the macropore and the matrix domain with the Richards' equation. Transfer of water between the two regions is simulated by means of a pressure-gradient-driven first-order rate equation:

$$\Gamma_w = \alpha_w(\psi_f - \psi_m) \tag{13a}$$

$$\alpha_w = \frac{\beta}{a_w^2} \gamma_w K_a \tag{13b}$$

where β is a factor depending on the geometry of the aggregates, a_w represents the distance from the centre of a fictitious matrix block to the fracture boundary, γ_w is an empirical coefficient, K_a the hydraulic conductivity of the exchange term and ψ_f and ψ_m the pressure heads in the macropore (and matrix domain resp.). *Figure 9c* shows the results of water infiltration after 0·1 and 0·3 d in a soil with hydraulic properties shown in *Figs 9a* and *b* and under the initial and boundary conditions given by Eqns (5a)–(5c). In comparison with the classical approach, water infiltrates deeper in the soil profile due to the higher conductivity through the macropores (*Fig. 9b*). However, since the matrix conductivity is lower, the matrix is not saturated except close to the surface and the transition zone is much more dispersed as compared with *Fig. 1c*.

Other approaches whereby water flow in the macropore region is described as a channelling flow[62,63] or a gravity-driven flow[64] can also be used to simulate preferential flow of water in micro-heterogeneous soils.

4.1.2. *Dual-porosity models for solute transport*

In a dual-porosity model, convective–dispersive solute transport takes place in both the macro- and micro-pore regions. Solute exchange between both regions is caused by interregion molecular diffusion and advection. The transport equations are given as[65,61]

$$\frac{\partial \theta_1 C_1}{\partial t} = \nabla \cdot (\theta_1 \mathbf{D}_1 \nabla C_1 - \theta_1 C_1 \mathbf{v}_1) - \Gamma_s \tag{14a}$$

$$\frac{\partial \theta_2 C_2}{\partial t} = \nabla \cdot (\theta_2 \mathbf{D}_2 \nabla C_2 - \theta_2 C_2 \mathbf{v}_2) + \Gamma_s \tag{14b}$$

$$\Gamma_s = \alpha_w(\psi_1 - \psi_2) C^* + \alpha_s(C_1 - C_2) \tag{14c}$$

$$C^* = C_1 \quad \text{if}\, (\psi_1 - \psi_2) > 0, \qquad C^* = C_2 \quad \text{if}\, (\psi_1 - \psi_2) < 0, \tag{14d}$$

with θ_i the volumetric water content in pore region i, relative to the total soil volume. The set of CDE equations describing solute transport in both the regions is coupled by the interaction term Γ_s. The first and second terms of Γ_s account for, respectively, the advective and dispersive exchange of solutes between both regions. The first-order advective transfer coefficient, α_w, depends on (1) the hydraulic conductivity of the interface between both regions, and (2) the size and shape of the matrix blocks according to Eqn (13b).[66] The first-order diffusive transfer coefficient, α_s, depends on (1) the effective molecular diffusion in the matrix blocks, and (2) the size and shape of the matrix blocks.[67] Simulated concentration profiles in a dual-porosity medium after 0·1 and 12·5 d of application are given for illustration in *Fig. 9d*. It is evident from *Fig. 9d* that the dual-porosity model predicts a very fast solute movement in the macropore region and that solutes in the macropore region "bypass" the matrix. However, the solute movement through the matrix is slower than that in the classical approach (*Fig. 1d*) due to the lower hydraulic conductivity in the matrix.

When coupled with a dual-porosity water flow model, this model can predict preferential solute transport in macroporous soils under non-steady flow conditions (e.g. Refs 64 and 68). An advantage of coupling the dual-porosity water flow equations with the dual-porosity solute transport equations is that critical parameters of the latter equations such as θ_i and v_i are output variables of the former equations.

4.2. *Stream tube and stochastic-continuum models for "macro-heterogeneous soils"*

Since solute transport in a heterogeneous three-dimensional variably saturated porous medium cannot be simulated using parameters determined at the local scale, several conceptual models have been developed to predict the field-scale solute transport in "macro-heterogeneous soils". The different approaches can be subdivided in two main classes: a deterministic approach and a stochastic approach. In the deterministic approach, either the heterogeneity of the soil is ignored and the heterogeneous medium is represented as an equivalent homogeneous one, or an exact picture of the observed heterogeneity for a particular site is generated. Since effective parameters for description of field-scale processes cannot be derived simply from taking the arithmetic averages of parameters that describe local-scale processes (e.g. Ref. 69), the former approach requires scale-up techniques that relate local-scale parameters to field-scale parameters taking into account the stochastic properties of the local-scale parameters. The other approach, the exact representation of the field-scale variability, requires a large amount of data that cannot be obtained.[70]

In contrast to the deterministic approach, stochastic models account explicitly for the variability of the soil properties which are viewed as random variables. Due to the stochastic nature of the soil properties, i.e. input parameters of transport models, the output variables of interest (e.g. drainage, pesticide leaching to groundwater) are also random variables. Two steps are involved in the stochastic approach: (1) the statistical characterization of the soil properties or input variables, and (2) the derivation of the statistical properties of the output variables from the statistical properties of the input variables.

4.2.1. *Characterization of spatial variability*

As mentioned above, macroscopic soil properties show a deterministic variability, $\mu(\mathbf{x})$ (= the vector of the deterministic components of all soil properties of interest at location $\mathbf{x}$), and a small-scale stochastic variability, $\varepsilon(\mathbf{x})$ (= the vector of the stochastic components of all soil properties of interest at location, $\mathbf{x}$) (*Fig. 10*). The stochastic component vector $\varepsilon(\mathbf{x})$ is described by a random space function, $Z(x)$, (RSF) which determines the means, variances, covariances of the stochastic components and the covariances between stochastic components at different locations. The latter covariances define the spatial structure of the small-scale stochastic heterogeneity. For a detailed description of the theory of RSFs, the reader is referred to Refs 71 and 72.

To reduce the number of probability density functions (p.d.f.) that are required to define the RSF, it is in general assumed that the stochastic components are second-order stationary: (1) the expected value or the mean of $\varepsilon(\mathbf{x})$ is constant in the field, and (2) the covariances between $\varepsilon(\mathbf{x}_1)$ and $\varepsilon(\mathbf{x}_2)$ are only a function of the distance between the two locations $\mathbf{h} = \mathbf{x}_1 - \mathbf{x}_2$ and not of the location in the field. In other words, for each separation vector $\mathbf{h}$, only one p.d.f. is used to define the covariances of all pairs $[\varepsilon(\mathbf{x}_1), \varepsilon(\mathbf{x}_2)]$ with $\mathbf{x}_1 - \mathbf{x}_2 = \mathbf{h}$.

Also the number of input parameters, i.e. the elements of the vector $\varepsilon(\mathbf{x})$ can be reduced drastically if the concept of scaling is used to describe the spatial variability of the soil hydraulic properties. The concept of scaling also simplifies the models discussed in the next sections with respect to their analytical development and/or to the computational effort. A first attempt was made by Miller and Miller,[73] who derived the relation between the pressure head (or hydraulic conductivity) of a particular medium with the pressure head (or hydraulic conductivity) of a reference medium assuming that both media have identical internal geometries and porosities. Such so-called Miller-similar media differ only in their characteristic length, a^*. These relations, derived from physical laws of surface water tension, are given by

$$\psi_r = (a_m/a_r)\psi_m \tag{15}$$

$$K_r = (a_r/a_m)^2 K_m \tag{16}$$

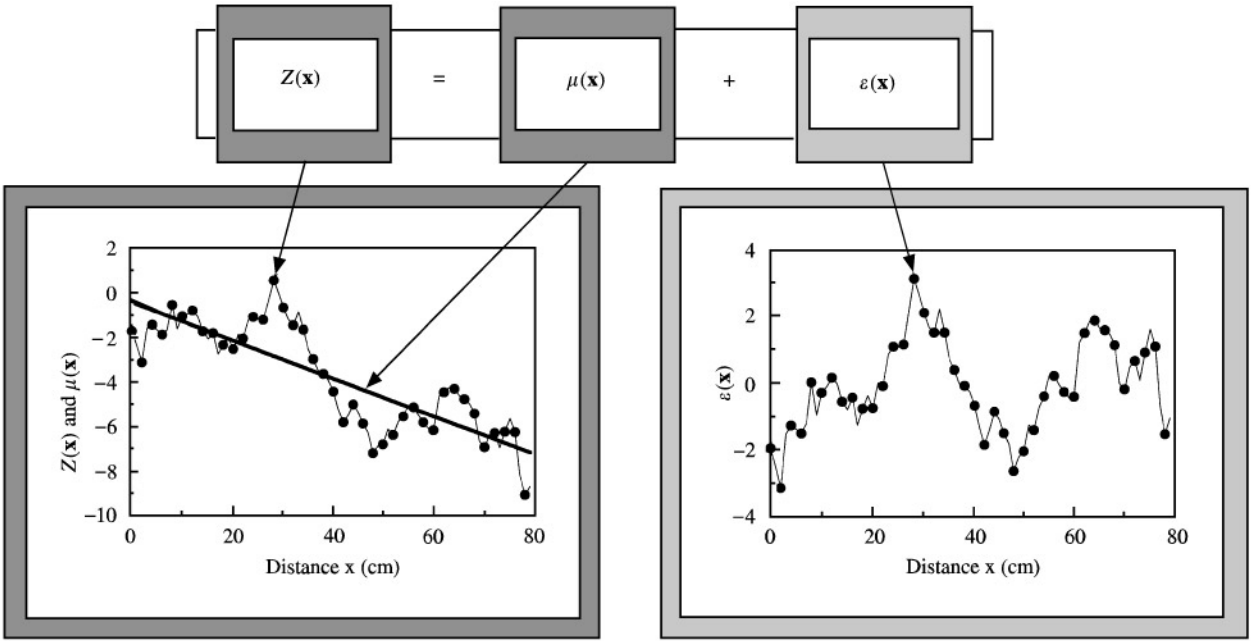

Fig. 10. Deterministic variability, $\mu(\mathbf{x})$, and small-scale stochastic variability, $\varepsilon(\mathbf{x})$, of a random space function, $Z(\mathbf{x})$

where the subscripts m and r indicate the reference and the scaled medium, respectively. The scaling factor a_r is defined as a_r^*/a_m^*. The derivation of scale factors based on physical laws is sometimes referred as dimensional analysis.[74]

However, to make the scaling concept more applicable, scale factors are obtained by relating the soil hydraulic function at different locations to an average soil hydraulic function, the so-called functional normalization.[74] Instead of assuming a strict Miller-similar medium, it is sufficient to assume functional similarity.[75] In fact, only the linear component of the spatial variability of the hydraulic functions is described by scaling factors,[76] e.g. the α and K_s parameters in Eqns (3) and (4). This means that scaling can only be applied as long as the non-linearity has only a small contribution to the total variability, e.g. the variability of n is low [Eqns (3) and (4)]. This means that the spatial variability of the hydraulic properties can be represented by linear translations of the reference functions $\psi^*(\theta)$ or $K^*(\theta)$:

$$\psi(\theta, \mathbf{x}) = a_1(\mathbf{x})\psi^*(\theta) \tag{17}$$

$$K(\theta, \mathbf{x}) = a_2(\mathbf{x})K^*(\theta) \tag{18}$$

with a_i^* a scaling factor which characterizes the stochastic nature of the hydraulic properties and $\mathbf{x}$ a vector containing the spatial coordinates. In *Fig. 11*, $\theta(\psi)$ before and after scaling are shown.[38] The scale factors were lognormal distributed as was also observed in the studies of Warrick *et al.*,[77] Hopmans[78] and Mallants *et al.*,[37] amongst others.

Figure 12a displays the bivariate p.d.f. of a_1 and a_2. To fully characterize the RSFs of the scaling factor, the covariance function is estimated (*Fig. 12b*).

4.2.2. *Prediction of effective parameters using stream tube models*

In this approach, the soil is conceptualized as a collection of stream tubes. Within each stream tube, water flow and solute transport are described with a certain transport model. There is no exchange of water and solutes between the stream tubes. The parameters determining the water flow and solute transport are viewed to be deterministic within a stream tube but vary between the stream tubes. In stream tube models, the spatial structure of the heterogeneity of soil properties or input parameters is not considered. The heterogeneity is represented by a single p.d.f. which determines the mean, variance and covariances of the input parameters which are observed at the same location.

One of the first stream tube models (STM) developed to describe the conservative solute transport was the so-called Bresler-Dagan model (BD model)[79,80] Solute particles are transported only by convection, thus neglecting the pore-scale dispersion. The solute particle velocity in a single stream tube is thus identical to the steady-state water flow in that stream tube. The water flow velocity in a stream tube is a function of the constant

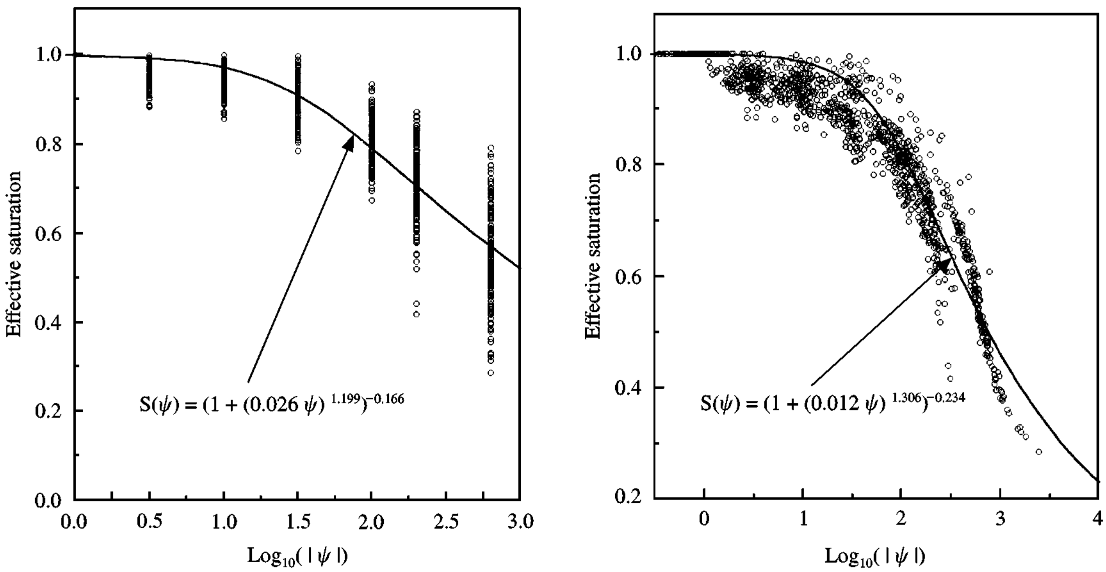

Fig. 11. Unscaled (left) and scaled (right) $\theta(\psi)$ data from a sandy-loam macroporous soil together with the fitted van Genuchten function. The ratio of the minimum mean-squared error after scaling to the mean-squared error before scaling was 0·877[38]

water recharge, q, at the soil surface (which is uniform over the domain) and the hydraulic properties of the stream tube. Since the hydraulic properties are random between the stream tubes, the solute particle velocities are also random.

If $K(\psi)$ is described with a parametric function, the water velocity can be expressed as a function of these parameters. In the BD model, the only random parameter taken into account is K_s and its variability is described with a lognormal-distributed scale factor. Consequently, the solute distribution in a heterogeneous field is described as a function of the p.d.f. of the scaling factor a_2.

More generally, the first moment of the output variable of interest, $T(z,t)$, is

$$\langle T(z,t)\rangle = \int_{-\infty}^{+\infty} \cdots \int_{-\infty}^{+\infty} T(z,t|\mathbf{y}) f_{\mathbf{Y}}(\mathbf{y})\, dy_1 \cdots dy_n \tag{19}$$

where $\langle T(z,t)\rangle$ is the first moment of $T(z,t)$, $f_{\mathbf{Y}}(\mathbf{y})$ is the multivariate p.d.f. of the input variables and $T(z,t|\mathbf{y})$ is the value of the output variable for the specific input variables $\mathbf{y}$. Similarly the variance of the output variable is given as

$$\mathrm{Var}[T(z,t)] = \int_{-\infty}^{+\infty} \cdots \int_{-\infty}^{+\infty} [T(z,t|\mathbf{y}) - \langle T(z,t)\rangle] f_{\mathbf{Y}}(\mathbf{y})\, dy_1 \cdots dy_n \tag{20}$$

If the transport process is simple, it can be solved analytically, whereas for complex transient transport processes, $T(z,t|\mathbf{y})$ should be solved using a numerical simulation model. In *Fig. 13a* ten realizations of K_s are shown. Each realization represents a stream tube, each with a different value for the K_s. These sream tubes were used as input in a numerical simulation model to calculate the infiltration in a soil under ponding conditions (*Fig. 13b*) and steady-state solute transport (*Fig. 13c*) subjected to the initial and boundary conditions given by Eqns (5a)–(5c) and (8a)–(8c), respectively.

A typical characteristic of a STM is that dispersion of a solute plume or of a field-scale-averaged BTC, D_{eff}, predicted by a STM increases linearly with the travel depth of the solute plume. This is in line with the behaviour of D_{eff} with increasing plume travel distance observed in several lysimeters (e.g. see Refs 81, 82 and 14) and field experiments (e.g. see Refs 83, 84 and 34).

We will discuss some examples of the STM. *Figure 14* shows the observed field-scale BTCs obtained from a steady-state *in situ* solute transport experiment in a loamy soil. The full lines represent the CDE [Eqn (6)] which is fitted to the field-scale-averaged BTC. The CDE parameters obtained from this fit represent "effective" parameters, v_{eff} and D_{eff}. Note that D_{eff} increases with increasing depth. In addition, the field-scale BTC predicted by Eqn (19)[84,85] based on the p.d.f. of the local-scale solute transport parameters v and D which are derived from CDE fits to local BTCs, is shown. In this particular case, the field-scale BTC, up scaled from local-scale BTC using a STM, matched the observed field-scale BTC perfectly.

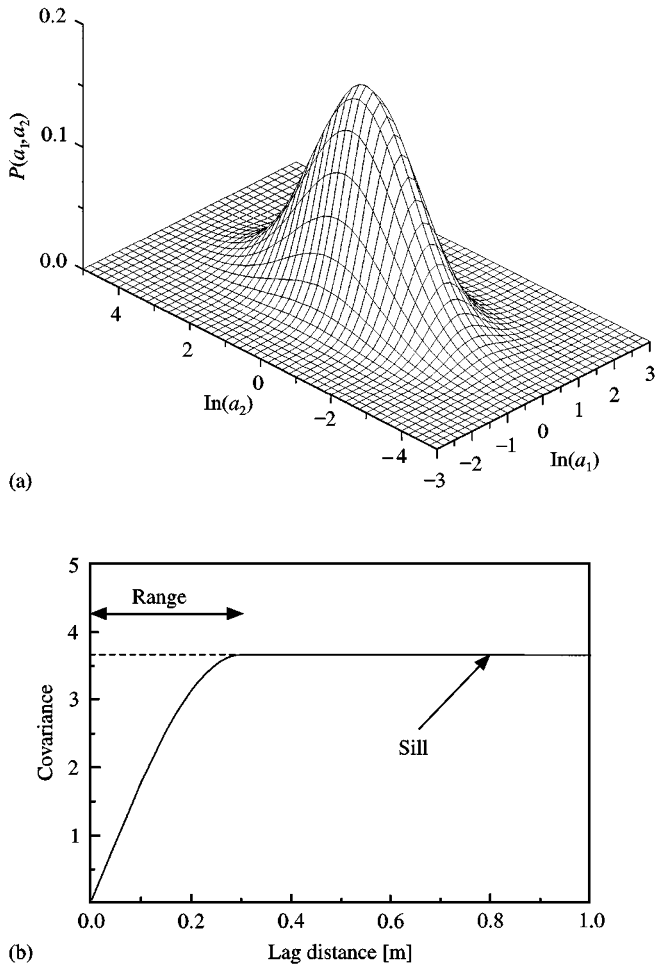

Fig. 12. (a) Bivariate normal distribution of $\ln(a_1)$ and $\ln(a_2)$ with mean = 0 for a_1 and a_2, and variance 0·668 and 3·67 for a_1 and a_1, respectively; (b) semi variogram for $\ln(a_2)$ with correlation length, l = 10 cm and sill = 3·67

Mallants *et al.*[18] determined the multivariate p.d.f. of the parameters of Eqns (3) and (4). Field-scale drainage of a macroporous, initially saturated soil was simulated in the STM framework by numerically solving the Richards' equation [Eqn (2)]. Compared with observed field-scale drainage, both the mean and the variability of the drainage were underestimated. The main reason was the inappropriate description of the hydraulic properties for this macroporous soil. Mallants *et al.*[60] found that a multi-modal model for $\theta(\psi)$ [Eqn (11)] improved the description of $\theta(\psi)$ significantly. In addition, the dual-porosity model discussed in Section 4.1.1 may describe better the water flow process in a macroporous soil.

The main purpose of the STM approach is to model solute transport at the field-scale using the p.d.f. of local-scale hydraulic parameters (BD model[86]). Under saturated flow conditions, when water is ponded on the soil surface, the STM predicts variable water fluxes in different stream tubes due to variations in K. For such a condition, field-scale solute transport can accurately be predicted using a STM.[29] For unsaturated flow conditions, the infiltration rate at the soil surface is nearly uniform and differences in solute velocity between different stream tubes are only explained by different water contents in the stream tubes. However, the observed coefficient of variation of θ is considerably smaller than the coefficient of variation of v[35] and a STM underestimates the field-scale solute dispersion for these conditions (e.g. Refs 40 and 34). To derive the variability of the solute velocity under unsaturated flow conditions from the heterogeneity of the hydraulic properties, horizontal water and solute redistribution must be accounted for. Therefore, a two- or three-dimensional description of water flow and solute transport is required which implies that the spatial structure of the soil heterogeneity has to be characterized.

4.2.3. *The stochastic-continuum approach*

By the stochastic-continuum approach, the flow and transport processes in a heterogeneous medium are modelled by the same continuum equations that are used in a homogeneous medium. The parameters of the flow and transport equations, and as a direct consequence also the variables, are stochastic functions in space or RSFs which represent the spatial heterogeneity of these parameters and variables. In order to apply the continuum equations, the scale of the heterogeneities of the hydraulic parameters should be much larger than the scale of the REV, the elementary soil volume over which the flow variables are averaged so as to obtain continuously varying variables in space.[87] The objective of the stochastic-continuum approach is to derive, from the stochastic properties (i.e. mean, variance and spatial correlation structure), of the water flow and solute transport parameters: (1) the stochastic properties of flow and transport variables (i.e. pressure head, water content, water flux, solute concentration, solute flux), and (2) "effective" flow and transport parameters which are constant in space and predict mean water flow and solute transport variables.

Two methodologies are followed to pursue these objectives. In the Monte-Carlo approach, heterogeneous fields, which are realizations of the RSF defining the flow and transport parameters in space, are generated using a random-field generator. In an alternative approach, analytical methods are used to solve the stochastic flow and transport equations.

4.2.3.1. *Monte-Carlo analysis.* A Monte-Carlo analysis involves two major steps: (1) the generation of a heterogeneous soil having the desired statistical properties and (2) the numerical solution of the flow and transport

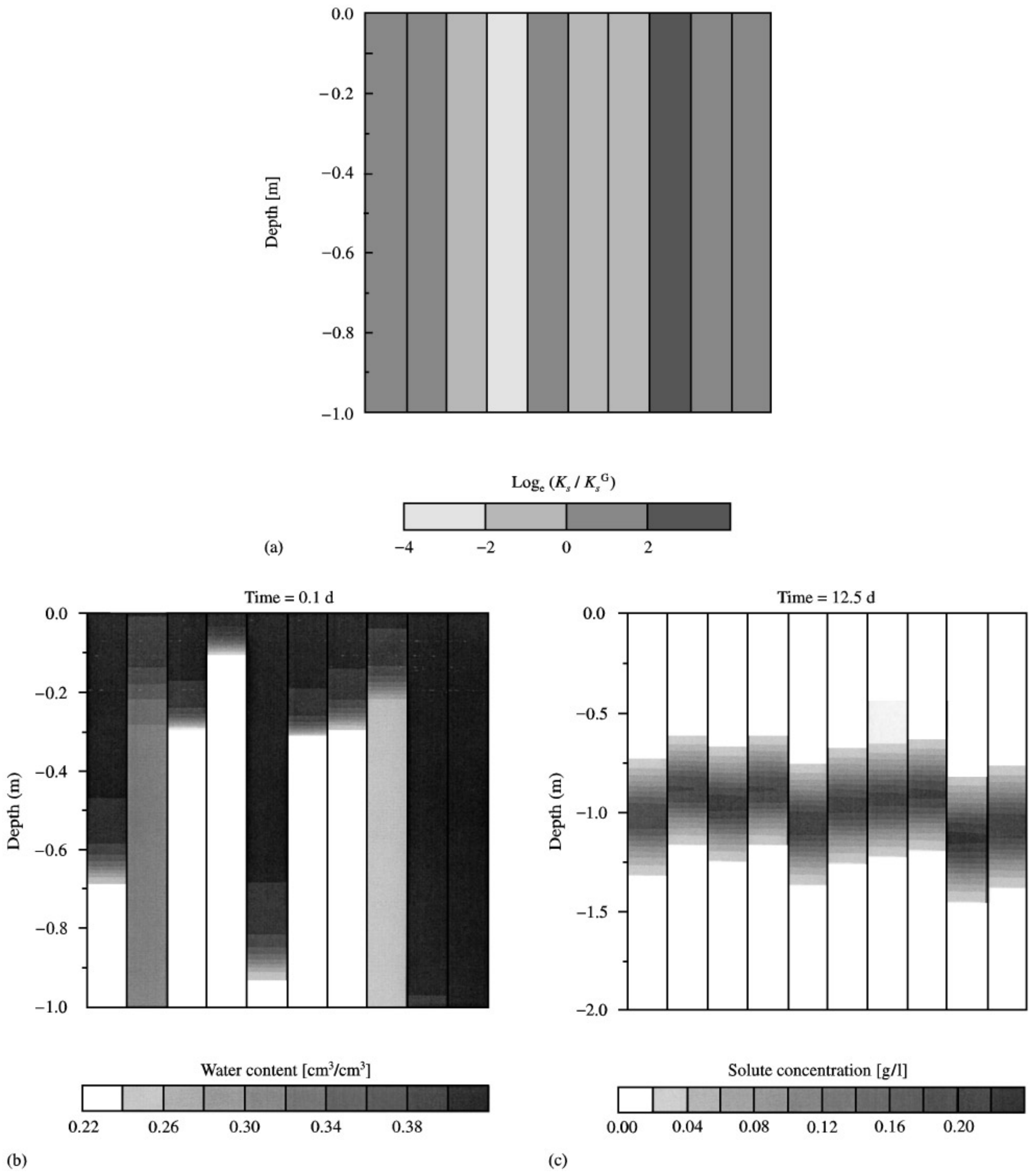

Fig. 13. (a) Ten stream tubes with different values of a_2 resulting from 10 realizations of a_2 (Fig. 12a) from the bivariate normal distribution; (b) water content profile after 0·1 d for boundary and initial conditions given by Eqns (5a)–(5c) using a STM;[79,80] (c) solute distribution at 12·5 d after solute application under steady-state flow conditions ($q = 2{\cdot}8$ cm/d) for boundary and initial conditions given by Eqns (8a)–(8c) using a STM[79,80]

equations in this generated soil. These steps can be repeated several times but, when relatively large heterogeneous fields, covering several correlation lengths of the fluctuations of the hydraulic properties, are generated, ergodicity can be invoked and the statistical properties of flow and transport variables can be derived from their spatial distribution in one realization of a random field.

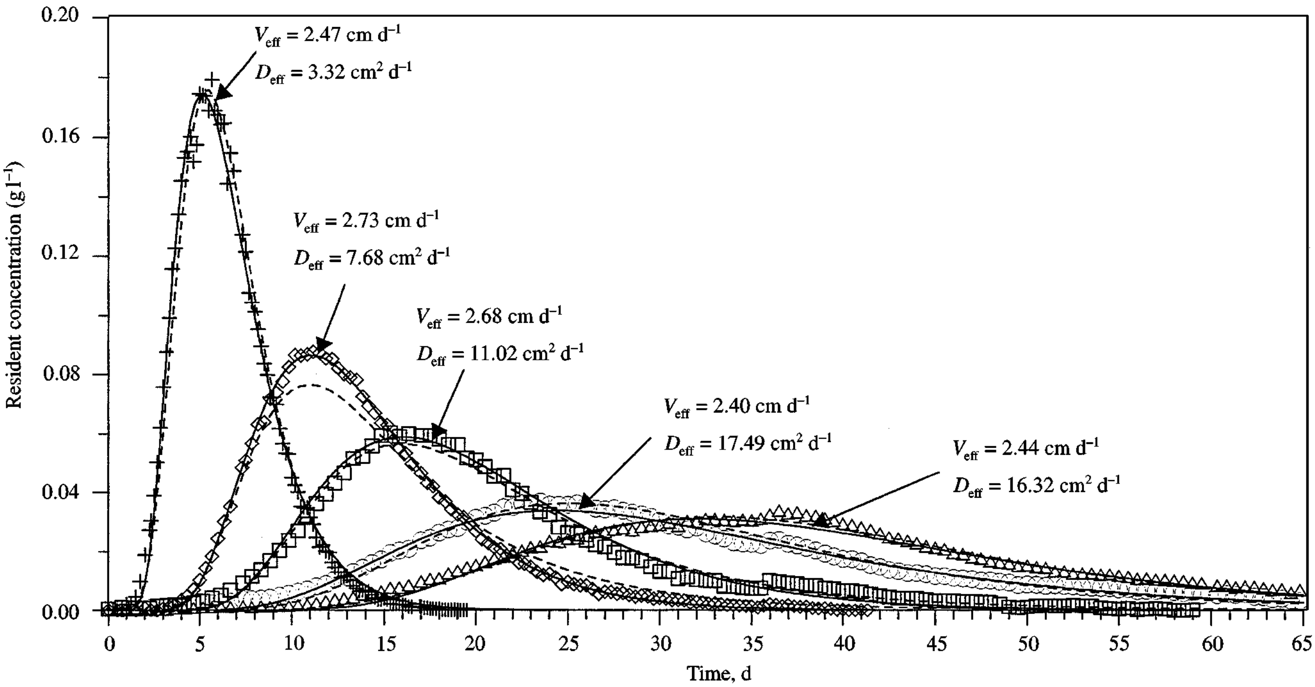

Fig. 14. Field-scale BTCs measured in situ during steady-state flow ($q = 1{\cdot}5$ cm/d) in a loamy soil together with fitted macroscopic CDE (full line), effective parameters of the macroscopic CDE, and predictions of field-scale BTCs using the STM of Toride and Leij:[84] —— *Macroscopic CDE;* ------- *STM; depth (cm)* + *15* ◇ 35 □ 50 ○ 70 △ *90*

Several methods exist to generate heterogeneous fields. A very computationally efficient method is the turning-bands method.[88] By this method, one-dimensional random line processes are generated which are subsequently projected to the multidimensional field. In another spectral method, randomization is done in the spectral domain based on the power and cross-spectral density structure of the random field.[89] The inverse Fourier transform of the random field in the spectral domain yields the random field in the spatial domain. An example of a heterogeneous field of K is given in *Fig. 15a*. The statistical information required is the mean, the variance and the correlation scale obtained from the covariance function (*Fig. 12b*).

To solve the Richards' equation numerically, finite-element and finite-difference schemes are used (e.g. SWMS_2D[90]). Since the hydraulic properties are interpolated or averaged between the computation nodes, the grid of computation nodes should be sufficiently small to avoid averaging out of the small-scale fluctuations of hydraulic properties. A minimal number of five nodes per correlation length of the soil hydraulic properties is suggested.[91] The solute transport equation can be solved numerically in two different ways: (1) using particle-tracking methods, and (2) using finite-element or finite-difference schemes. In the particle-tracking method, the continuous movement of the particles is discretized in time. Solute plumes or BTCs are obtained by recording the movement of large sets of particles. For each successive time step, the particle displacement is calculated based on its velocity during that time step. To account for local-scale dispersion, a random, zero-mean displacement is added to the advective displacement at each time step. The variance of the random displacement depends on the local-scale dispersion. The velocities at successive time steps can be derived from the spatial covariance of the velocity and from the velocities at previous time steps which condition the particle velocities at later time steps.[92] When local velocities are obtained after solving the flow equation, these velocities can be used directly in the particle-tracking procedure.[93,94]

To solve the transport equation using finite-element or finite-difference schemes, sufficiently small time and space increments should be used to avoid oscillatory behaviour of the numerical solution. The higher the advective solute flux as compared with the dispersive solute flux, the smaller the grid size and the time steps should be chosen to avoid numerical oscillations.[95,96,90] Especially when water flow is very heterogeneous resulting in high water fluxes at certain locations, finite-element or finite-difference schemes require a large computational effort.

The generated heterogeneous field of *Fig. 15a* is used as input in a numerical finite-element model (SWMS_2D[90]) to simulate water infiltration [initial and

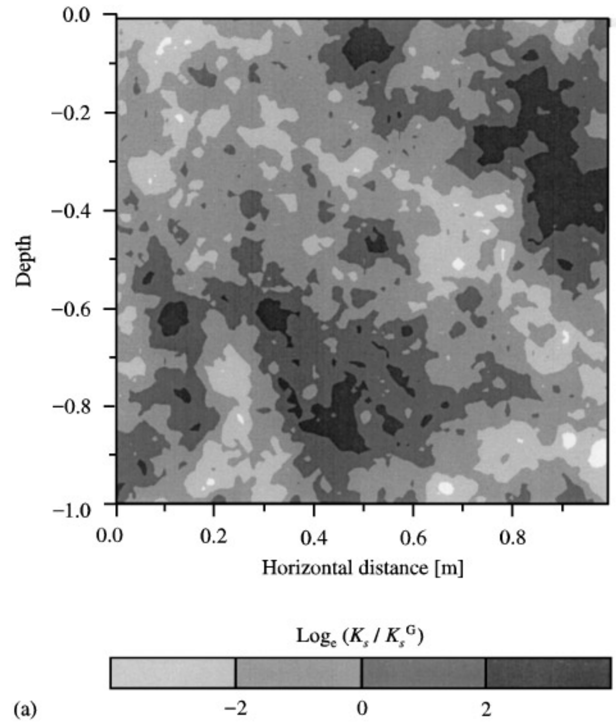

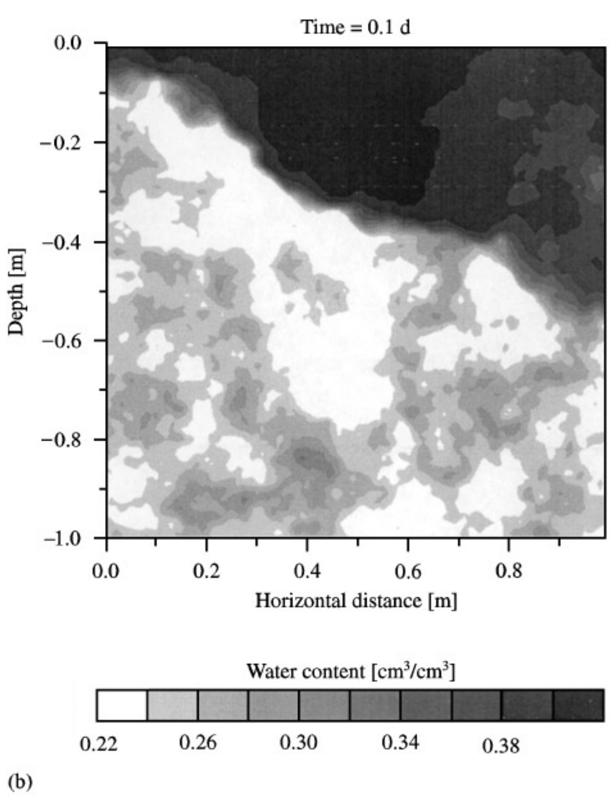

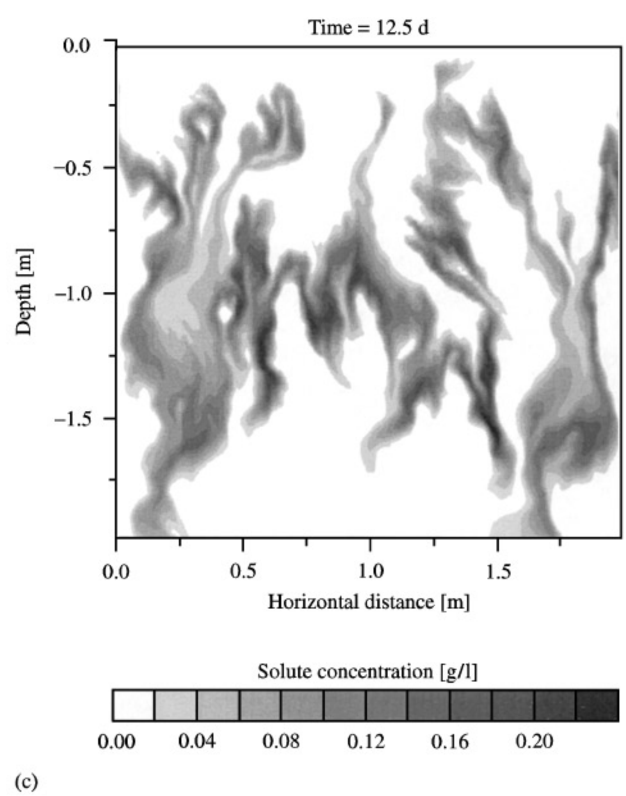

Fig. 15. (a) Random (heterogeneous) field generation of the hydraulic conductivity from the covariance function given in Fig. 12(b); (b) water content profile after 0·1 d for boundary and initial conditions given by Eqns (5a)–(5c) using SWMS_2D;[90] *(c) solute distribution at 12·5 d after solute application under steady-state flow conditions ($q = 2{\cdot}8$ cm/d) for boundary and initial conditions given by Eqns (8a)–(8c) using SWMS_2D*[90]

boundary conditions, Eqns (5a)–(5c), and solute transport (initial and boundary conditions, Eqns (8a)–(8c)]. In *Fig. 15b*, we see that the infiltration front varies clearly in the horizontal direction. The deeper infiltration on the right-hand side is due to the zone of higher conductivity values on the right-hand side in the generated hydraulic conductivity field (*Fig. 15a*). The solute concentration profile (*Fig. 15c*) is very irregular so that when solute concentrations are averaged along the horizontal direction, the average concentration profile is much more dispersed than for the case of solute transport in a homogeneous soil using the same local dispersivity (*Fig. 1d*).

Monte-Carlo simulations in two-dimensional heterogeneous fields are frequentely used with hypothetical input parameters to investigate the characteristics of solute transport in physically heterogeneous soil profiles and to evaluate other model approaches such as STM or the analytical models discussed in the next section.[97–99,48] However, comparison between two-dimensional Monte-Carlo simulations and field-scale water flow and solute transport are hard to find in the present literature. The reason is simply that the necessary input data, that is, detailed characterization of the spatial variability of the hydraulic properties and validation data from a detailed field-scale transport experiment on the same site are rare. We will discuss shortly two simulation excercises described recently in the literature.

Rockhold *et al.*[100] simulated the infiltration of water and tritium in an initially drained soil profile at the Las Cruces Trench Site.[101]. The spatial variability of hydraulic properties was characterized using scaling factors. *In situ* measured water contents at the start of the experiment were used to condition the heterogeneous field of the scaling factors. Instead of generating a random field using the techniques described above, Rockhold *et al.*[100] interpolated the scaling factors between the conditioned data. Simulated water and solute profiles matched the observed profiles quite well without any model calibration. A second example treats the simulation study of Vanderborght *et al.*[49] based on a steady-state solute transport experiment in a loam soil.[41] Hydraulic properties were measured on undisturbed soil samples of different sizes using different techniques.[37] The observed variance of the scaling factors depended largely on the measurement method. Consequently, random fields based on the different techniques showed different degrees of variability resulting in different simulated field-scale BTCs. This sensitivity of the outcome of the simulations with respect to the used measurement technique means that further evaluation of measurement techniques and simulations is absolutely required.

4.2.3.2. *Analytical method*

4.2.3.2.1. Water flow. The pertubation-spectrum analysis has been extensively used by various authors to solve the stochastic water flow equation (e.g. Refs 102–105). For steady-state conditions, the stochastic water flow equation is

$$\nabla\cdot(\mathbf{K}(\mathbf{x},\psi(\mathbf{x}))\nabla(\psi(\mathbf{x})+z))=0 \tag{21}$$

where $\mathbf{x}$ is the spatial coordinate and $\mathbf{K}(\mathbf{x},\psi(\mathbf{x}))$ and $\psi(\mathbf{x})$ are RSF. To simplify the solution of Eqn (21), the hydraulic conductivity is related to the pressure head by means of the exponential Gardner[5] equation:

$$\mathbf{K}(\mathbf{x},\psi(\mathbf{x}))=\mathbf{K}_s(\mathbf{x})\exp(\alpha(\mathbf{x})\psi(\mathbf{x})) \tag{22}$$

where $\mathbf{K}_s$ is the saturated hydraulic conductivity and α a parameter that characterizes the pore size distribution. Note that $\psi(\mathbf{x})$ is negative since $\psi(\mathbf{x})$ represents the capillary suction heads. Assuming that the local hydraulic conductivity is isotropic, the following equation is obtained after expanding and dividing Eqn (22) by $K(\mathbf{x},\psi(\mathbf{x}))$ $(K(\mathbf{x},\psi(\mathbf{x})))\mathrm{I}=\mathbf{K}(\mathbf{x},\psi(\mathbf{x}))$ with $\mathbf{I}$ being the unity matrix):

$$\nabla^2(\psi)+\nabla\cdot((\ln K_s+\alpha\psi)\nabla(\psi))+\frac{\partial(\ln K_s+\alpha\psi)}{\partial z}=0 \tag{23}$$

Next, $\ln K_s$, α, and ψ are expressed in terms of means and perturbations:

$$\psi=H+h,\qquad E(\psi)=H,\qquad E(h)=0 \tag{24a}$$

$$\alpha=A+a,\qquad E(\alpha)=A,\qquad E(a)=0 \tag{24b}$$

$$\ln K_s=Y+y,\qquad E(\ln K_s)=Y,\qquad E(y)=0 \tag{24c}$$

After substitution of Eqn (24) into Eqn (21) with Y and A assumed to be constant, the following relation is obtained after neglecting the products of perturbation quantities and assuming an average vertical unit hydraulic gradient:[104]

$$\nabla^2 h+A\frac{\partial h}{\partial z}+\frac{\partial y}{\partial z}+H\frac{\partial a}{\partial z}=0 \tag{25}$$

It should be noted that the first-order perturbation analysis is only applicable for soil property variances smaller than unity. For larger variances, the products of perturbation quantities cannot be neglected.

By means of Eqn (25), the pressure head fluctuations, h, are related to the fluctuations of the hydraulic properties of the heterogeneous field: a and y. Using Fourier–Stieltjes representations of the second-order stationary RSFs which define h, y, and a, in combination with the spectral representation theorem produces the relationship between the spectra of the fluctuations from which the spectrum of h fluctuations, S_{hh}, is derived. The Fourier transform of S_{hh} yields the autocovariance function of the head fluctuations. For a deterministic α and an isotropic field, the variance of the pressure heads $\sigma^2(\psi)$, is given as

$$\sigma^2(\psi) = \frac{\sigma^2(y)l^{*2}}{\alpha l^*}\left(1 - \frac{2\ln(1+\alpha l^*)}{\alpha l^*} + \frac{1}{1+\alpha l^*}\right) \quad (26)$$

where l^* is the correlation length of y. An analoguous procedure is followed to derive the stochastic properties of the water flux fluctuations.

The effective hydraulic conductivity $\mathbf{K}_{eff}$ is derived from the ratio of the mean water flow divided by the hydraulic gradient in the direction of the water flow.[104,105] For a deterministic α, a unit mean vertical pressure head gradient, and an isotropic field, K_{eff} is given as

$$K_{eff} = \exp(Y)\exp\left(\alpha H + \frac{\sigma^2(y)}{6}\right) \quad (27)$$

In a series of papers, Mantoglou and Gelhar[106–108] expanded this approach to transient flow conditions. The effective conductivities show a large-scale hysteresis, i.e. dependency of K_{eff} on the flow conditions (i.e. drying, wetting, steady-state) and a large-scale anisotropy depending on the flow condition and the mean hydraulic head in the soil. Since it was assumed that the local-scale hydraulic properties are non-hysteretic and isotropic, the hysteresis and the anisotropy of the effective conductivities originate from the spatial variability of the local-scale hydraulic properties. Mantoglou and Gelhar[106–108] discussed in detail these results of the stochastic theory and confronted them with field and laboratory observations which indicate a qualitative agreement between the stochastic theory and the observations. One practical consequence is that the predicted movement of the soil moisture plume calculated with effective conductivities of the stochastic theory will tend to spread out more laterally and less vertically compared with its predicted movement if simple averages of local hydraulic parameters are used.

Again, confrontation between stochastic simulations and field observations are rare in the present literature. Monte-Carlo simulations are sometimes used to validate the results of the stochastic theory. For example, Polmann *et al.*[109] evaluate the stochastic theory using a detailed numerical simulation of water flow. Tension profiles predicted with the stochastic theory were in good agreement with detailed simulations. Also ohter aspects of the stochastic theory, variance of tension, hysteresis and anisotropy of effective conductivities, were confirmed by the simulations. However, the statistical parameters of local-scale hydraulic properties were exactly known, whereas, in real field applications, they should be obtained from a few collected soil samples. Jensen and Mantoglou[110] compared the measured water content and pressure head under natural boundary conditions with predictions based on the stochastic theory. Statistical input parameters were obtained from measured hydraulic properties at soil samples from the same site. Reasonably good agreement between predictions and observations was obtained both for the mean response and the variance. Although this example illustrates the capacities of the stochastic theory to predict mean water flow from mesurements of local-scale hydraulic properties, more quantitative validation experiments are absolutely necessary.

4.2.3.2.2. Solute transport. The results of the stochastic water flow equation, i.e. the variance and correlation scales of the water flux fluctuations, are used to derive "effective" or "macro"-dispersion coefficients that describe the spreading of the solute plume or the BTC in a heterogeneous soil. Two approaches exist to derive the field-scale dispersion. In a first approach, the mean transport equation is evaluated by taking the expectation of the local stochastic transport equation.[111,112]

In a second approach, solute transport is described as "dispersion by continuous motions".[9,113] The displacement covariance tensor of solute particle positions at a time t or the variance of the solute particle arrival time at a certain depth z is calculated from the statistics of the velocity field using a Lagrangian formulation. The location of a particle that was added to the soil at location $\mathbf{x}_0$ and time t_0 at a time t is given as a function of the velocity that a particle experiences along its travel path (Langrangian velocity) as

$$\mathbf{x}(t) = \int_{t_0}^{t} \mathbf{v}(\xi(t), \mathbf{x}_0)\, dt \quad (28)$$

where $\mathbf{v}(\xi, \mathbf{x}_0)$ is the particle velocity and ξ the coordinates of the travel path. When the velocity fluctuations are stationary, and the local-scale dispersion is neglected, the covariance matrix of the particle locations, $\Sigma_{\mathbf{x}}(t)$, can be written in terms of the spatial correlation of the velocities approximately as

$$\begin{aligned}\sigma^2_{Xij}(t) &= 2\sigma^2_{vi\,vj}\int_{t_0}^{t}(t-t')\rho_{vi\,vj}(E(\mathbf{v})t')\,dt' \\ &= \frac{2\sigma^2_{vi\,vj}}{E(v)^2}\int_{z_0}^{z(t)}(z(t)-z(t)')\rho_{vi\,vj}(z(t)')\,dz(t)' \end{aligned} \quad (29)$$

where $z(t)$ is the mean location of the solute plume at time t, $\sigma^2_{Xij}(t)$ the ij entry of $\Sigma_{\mathbf{x}}$, $\sigma^2_{vi\,vj}$ the ij entry of the velocity covariance matrix, and $\rho_{vi\,vj}(\mathbf{x})$ the spatial (cross) correlogram between the ith and jth component of the velocity vector. A similar first-order approximation of the solute particle travel path is used to derive the variance of solute particle arrival times at a certain depth from the stochastic properties of the velocity field.[114–116,97] Based on moment analysis, the *ij* entries of the effective dispersion tensor, $\mathbf{D}_{eff}$, are related to $\sigma^2_{Xij}(t)$ as

$$D_{ij} = \frac{1}{2}\frac{\partial \sigma^2_{Xij}(t)}{\partial t} \tag{30}$$

From Eqns (29) and (30) it follows that $\mathbf{D}_{eff}$ is a function of (1) time or average travel depth of the solute plume, (2) the variance of the advection velocity and (3) the spatial correlation of the velocity fluctuations. Since the statistical properties of the velocity fluctuations can be related to the statistical properties of the hydraulic parameters, the effective dispersion coefficient can be derived directly from the statistical properties of the hydraulic parameters. Close to the input surface when the travel depth of the solute plume is smaller than the correlation length of $\ln(K_s)$, l^*, the longitudinal dispersion (the dispersion that quantifies the solute spreading in the direction of the mean solute flow) increases linearly with increasing travel depth. For saturated flow conditions and an isotropic random field the longitudinal dispersion is given as

$$D_{eff}(z) \approx \lambda_L v + \tfrac{8}{15}\sigma^2(y)vz \tag{31}$$

where v is the average pore water velocity and z the average travel depth.

When the travel depth is much larger than l^*, D_{eff} remains constant with depth and is given for saturated flow conditions and an isotropic random field as

$$D_{eff}(z) \approx \lambda_L v + \sigma^2(y)vl^* \tag{32}$$

This indicates that the correlation length of the soil property fluctuations is a critical parameter which determines the range of depths for which a stochastic stream tube model can be used to predict solute transport in soils. It also determines the critical travel depth below which solute transport can be described by a macroscopic convection–dispersion model with a constant dispersion parameter.

Since the variance and correlation length of the velocity fluctuations, which determine $\mathbf{D}_{eff}$, depend in a complex manner on (1) the variance, spatial correlation and intercorrelation of the soil properties and (2) on the mean water flow rate, water saturation, and pressure head, $\mathbf{D}_{eff}$ will also depend on these soil properties and flow variables. For instance, for steady-state vertical water flow (unit mean hydraulic head gradient), the longitudinal dispersivity, λ_L, increases with decreasing water saturation for soils in which α and $\ln(K_s)$ are not or negatively correlated.[117] When α and $\ln(K_s)$ are positively correlated, λ_L decreases with decreasing water saturation until a critical saturation degree is reached. Below this critical saturation degree, λ_L increases with decreasing degree of saturation.[117,48]

These results are in contradiction to the experimentally observed drastic increase of solute dispersivity with increasing flow rate or saturation degree in structured soils. As mentioned above, this increase was explained by the activation of large pores at higher flow rates. This opposite behaviour with increasing water flow or saturation degree of water flow and solute transport heterogeneity predicted by the stochastic-continuum approach and by dual-porosity models is explained by the implicit assumptions made in the stochastic-continuum approach. First, it is assumed that local-scale transport can be described by the continuum equations and that local-scale hydrodynamic dispersivity is independent of the flow rate. Second, it is assumed that close to saturation, the coefficient of variation of the hydraulic conductivity is independent of the pressure head which is in contradiction to the drastic increase of this coefficient of variation with increasing saturation degree in structured soils.[118]

Based on the theoretical analysis of the stochastic transport equation, it can be concluded that in order to use a one-dimensional macroscopic or field-scale convection–dispersion model to model field-scale solute transport, the effective longitudinal dispersivity should be adjusted with travel depth and water saturation degree or flow rate. As a result, the classical assumption of a constant dispersivity which is independent of the travel depth and flow rate cannot be invoked.

5. Conclusions

Giving the growing concern about the quality of the environment, many scientists and decision makers are interested in a quantitative description of the water flow and the transport of pollutants in the soil. From the beginning of this century, soil physicists have been trying to describe water flow and solute transport in porous media or soils based on physical laws using a mathematical framework. However, most of their work was restricted to homogeneous soils. Although it provided many useful insights into the flow and transport phenomena, their solutions may not be adequate for describing transport processes in natural soils under field conditions. The major problem in many soils is the discrepancy between the assumption of a homogeneous porous medium and the observed heterogeneity, both at the micro- and macro-scale. Micro-heterogeneity, occurring in structured, cracked or macroporous soils, and macro-heterogeneity, due to the inherent spatial variability of soil properties, have a distinct effect on the water flow and solute transport processes. Solutions for environmental water flow and solute transport problems require adapted modelling concepts including the specific transport processes occurring in heterogeneous fields.

In this paper, we discussed some recent modelling concepts dealing with the description of water flow and solute transport in heterogeneous soils. These models are also based on physical laws and are expressed using the same mathematical framework as in the classical approach. However, they are formulated in a way that the effects of soil heterogeneity are accounted for. Preferential solute transport through heterogeneous soils is described using the dual-porosity concept. The macro-heterogeneity of the soil is represented by a statistical model of spatial variability. The statistical parameters are subsequently used to derive the statistical parameters of the flow and transport variables at the field scale.

However, before the discussed models can be used to solve some specific environmental or management problems, they should be validated extensively. This requires detailed experiments of water flow and solute transport for different initial and boundary conditions in a range of different soil types. In addition, research is needed to optimise measurements techniques which identify the necessary model parameters.

These models are well described in the present literature. It is not an overwhelming job to incorporate other processes such as a reactive solute transport. An important extension of the existing models is the combination of micro- and macro-heterogeneity in one mathematical framework. Since macropores act as preferential flow paths, occurrences of macropores at the field scale may enlarge the risk of leaching of pollutants to the groundwater. Therefore, a quantitative prediction of solute transport in macroporous (i.e. micro-heterogeneity) soils at field or regional scales (i.e. macro-heterogeneity) is an important matter in dealing with environmental problems.

Acknowledgements

The second and the third authors are research assistants of the Flemish Institute for the Encouragement of Scientific-Technological Research in the Industry (IWT). The last author is a research assistant of the Belgian National Fund for Scientific Research (F.W.O.). The authors would like to acknowledge the respective funding agencies.

References

1 **Bear J** Dynamics of Fluids in Porous Media. New York: Elsevier, 1972

2 **Richards L A** Capillary conduction of liquids through porous media. Physics, 1931, **1,** 318–333

3 **van Genuchten M Th** A closed-form equation for predicting the hydraulic conductivity of unsaturated soils. Soil Science Society of America Journal, 1980, **44,** 892–898

4 **Mualem Y** A new model for predicting the hydraulic conductivity of unsaturated porous media. Water Resources Research, 1976, **12,** 513–522

5 **Gardner W R** Some steady state solution of the unsaturated moisture flow equation with application to evaporation from a water table. Soil. Science, 1958, **85,** 228–232

6 **Gilham R W; Klute A; Herman D F** Hydraulic properties of a poreus medium. Measurements and empirical representations. Soil Science Society of America Journal, 1976, **40,** 203–207

7 **Brooks R H; Corey A T** Hydraulic properties of porous media. Hydrology Paper No. 3, Colorado State University, Fort Collins, Colorado, 1964, 27Pp

8 **Vanclooster M; Viaene P; Diels J; Christiaens K** Water and Agrochemicals in the soil and the Vadose Environment. Reference and User's Manual. Release 2.0. Institute for Land and Water Management, K.U. Leuven, Belgium, 1994, 139Pp

9 **Dagan G** Flow and Transport in Porous Formations, New York: Springer, 1989

10 **Beese F; Wierenga P J** The variability of the apparent diffusion coefficient in undisturbed soil columns. Zeitschrift für Pflanzenernährung und Bodenkunde, 1983, **146,** 302–315

11 **Pfannkuch H O** Contribution à l' étude des déplacements de fluides miscibles dans un milieu poreux (Contribution on the study of the displacement of immiscible fluids in a porous medium) Revue de l'Institut Français du Pétrole, 1963, **18,** 215–270

12 **Skopp J; Gardner W R** Miscible displacement: an interacting flow region model. Soil Science Society of America Journal, 1992, **56,** 1680–1686

13 **Dyson J S; White R E** The effect of irrigation rate on solute transport in soil during steady state water flow. Journal of Hydrology, 1989, **107,** 19–29

14 **Vanderborght J; Gonzales C; Vanclooster M; Feyen J** Effects of soil type and water flux on solute transport. Soil Science Society of America Journal, 1997, **61,** 372–389

15 **Beven K; Germann P** Macropores and water flow in soils. Water Resources Research, 1982, **18,** 1311–1325

16 **White R E** The influence of macropores on the transport of dissolved and suspended matter through soil. Advances in Soil Science, 1985, **3,** 95–121

17 **Bouma J** Influence of soil macroporosity on environmental quality. Advances in Agronomy, 1991, **46,** 1–37

18 **Mallants D; Jacques D; Vanclooster M; Diels J; Feyen J** A stochastic approach to simulate water flow in a macroporous soil. Geoderma, 1996, **70,** 299–324

19 **Bouma J** Soil morphology and preferential flow along macropores. Agricultural Water Management, 1981, **3,** 235–250

20 **Trojan M D; Linden D R** Microreliëf and rainfall effects on water and solute movement in earthworm burrows. Soil Science Society of America Journal, 1992, **56,** 727–733

21 **Wildenschild D; Jensen K H; Villholth K; Illangasekare T H** A laboratory analysis of the effect of macropores on solute transport. Ground Water, 1994, **32,** 381–389

22 **Smettem K R J; Collis-George N** Statistical characterization of soil biopores using a soil peel method. Geoderma, 1985, **36,** 27–36

[23] **Ghodrati M; Jury W A** A field study using dyes to characterize preferential flow of water. Soil Science of America Journal, 1990, **54,** 1558–1563

[24] **Timmerman A; Vanderborght J; Mallants D; Jacques D; Feyen J** Detecting Macropore flow in the field with TDR and staining patterns. In Annales Geophysica, Procedings of the XXIth General Assembly of the European Geophysical Society, The Hague, 6–10 May 1996, 237

[25] **Timmerman A; Feyen J** Measurement of near-saturated hydraulic conductivity in a macroporous soil. In European Workshop on Advanced Methods to Determine Hydraulic Properties of Soils, Thurneau, Germany, 9–12 June 1996, 7–10

[26] **Vanderborght J** Experimental and numerical study on nonreactive solute transport in soils. PhD dissertation, no. 349 of the Faculteit Landbouwkundige en Toegepaste Biologische Wetenschappen, Katholieke Universiteit Leuven, Belgium, 1997

[27] **Bowman R S; Rice R C** Transport of conservative tracers in the field under intermittent flood irrigation. Water Resources Research, 1986, **22,** 1531–1536

[28] **Dyson J S; White R E** A comparison of the convection-dispersion equation and transfer function model for predicting chloride leaching through an undisturbed structured clay soil. Journal of Soil Science, 1987, **38,** 157–172

[29] **Jaynes D B; Bowman R S; Rice R C** Transport of a conservative tracer in the field under continuous flood irrigation. Soil Science Society of America Journal, 1988, **52,** 618–624

[30] **Nielsen D R M Th; van Genuchten; J W Biggar** Water flow and solute transport processes in the unsaturated zone. Water Resources Research, 1986

[31] **Schulin R; van Genuchten M Th; Flühler H; Ferlin P** An experimental study of solute transport in a stony field soil. Water Resources Research, 1987, **23,** 1785–1794

[32] **Flury M; Leuenberger J; Studer B; Flühler H** Transport of anions and herbicides in a loamy and a sandy field soil. Water Resources Research, 1995, **31,** 823–835

[33] **Ritsema C J; Dekker L W; Dekker J M H; Hamminga W** Preferential flow mechanism in a water repellent sandy soil. Water Resources Research, 1993, **29,** 2183–2193

[34] **Jacques D; Vanderborght J; Mallants D; Kim D -J; Vereecken H; Feyen J** Evaluation of three stream tubes predicting field scale transport. Hydrology and Earth System Sciences, 1998 (in press)

[35] **Jury W A** Spatial variability of soil physical parameters in solute migration: A critical literature review. EPRI EA-4228 Project 2485-6, Riverside, CA, 1985

[36] **Byers E; Stephens D** Statistical and stochastic analysis of hydraulic conductivity and particle size in a fluvial sand. Soil Science Society of America Journal, 1983, **47,** 1072–1080

[37] **Mallants D; Jacques D; Tseng P H; van Genuchten M Th; Feyen J** Comparison of hydraulic property measurement methods. Journal of Hydrology, 1997, **199,** 295–318

[38] **Jacques D; Vanderborght J; Mallants D; Mohanty B P; Feyen J** Analysis of solute redistribution in heterogeneous soil: I. Geostatistical approach to describe the spatial scaling factors. In geoENV I–Geostatistics for Environmental Applications (Soarez A *et al.* eds) Pp. 271–282. The Netherlands: Kluwer Academic Publisher, 1997

[39] **Ellsworth T R; Jury W A; Ernst F F; Shouse P J** A three-dimensional field study of solute transport through unsaturated, layered, porous media. 1. Methodology, mass recovery, and mean transport. Water Resources Research, 1991, **27,** 951–965

[40] **van Weesenbeeck I J; Kachanoski R G** Effect of variable horizon thickness on solute transport. Soil Science Society of America Journal, 1994, **58,** 1307–1316

[41] **Feyen J; Diels J; Kim D -J; Vanclooster M; Hubrechts L** Assessment of the effects of climate and land use change on the physical and the physico-chemical soil properties and on the transfer and fate of soil water and chemical compounds. Internal Publication no. 46, Institute of Land and Water Management, Katholieke Universiteit Leuven, 1995, 116Pp.

[42] **Nielsen D R; Biggar J W; Erh K T** Spatial variability of field measured soil water properties. Hilgardia, 1973, **42,** 215–259

[43] **Ünlü K; Kavvas M L; Nielsen D R** Stochastic analysis of field measured unsaturated hydraulic conductivity. Water Resources Research, 1989, **25,** 2511–2519

[44] **Russo D; Buoton M** Statistical analysis of spatial variability in unsaturated flow parameters. Water Resources Research, 1992, **28,** 1911–1925

[45] **Mallants D; Mohanty B P; Jacques D; Feyen J** Spatial variability of hydraulic properties in a multi-layered soil profile. Soil Science, 1996, **161,** 167–181

[46] **Russo D** Stochastic analysis of simulated vadose zone solute transport in a vertical cross section of heterogeneous soil during nonsteady water flow. Water Resources Research, 1991, **27,** 267–283

[47] **Tseng P H; Jury W A** Comparison of transfer function and deterministic modeling of area-averaged solute transport in a heterogeneous field. Water Resources Research, 1994, **30,** 2051–2063

[48] **Roth K; Hammel K** Transport of conservative chemical through an unsaturated two-dimensional Miller-similar medium with steady state flow. Water Resources Research, 1994, **32,** 1653–1663

[49] **Vanderborght J; Jacques D; Mallants D; Tseng P H; Feyen J** Analysis of solute redistribution in heterogeneous soil: II. Numerical simulation of solute transport. In geo ENVI - Geostatistics for Environmental Applications (Soarez et al. eds.) pp. 283–295. The Netherlands, Kluwer Academic Publishers, 1997

[50] **van Weesenbeeck I J; Kachanoski R G** Spatial scale dependency of *in situ* solute transport. Soil Science Society of America Journal, 1991, **55,** 3–7

[51] **Elrick D E; Reynolds W D** Infiltration from constant-head well permeameters and infiltrometers. In Advances in Measurements of Soil Physical Properties: Bringing Theory into Practice (Topp G C; Reynolds W D; Green R E eds), Pp. 1–24. SSSA Special Publication no. 30, 1992

[52] **Booltink H W G; Bouma J; Giménez D** Suction crust infiltrometer for measuring hydraulic conductivity of unsaturated soil near saturation. Soil Science Society of America Journal, 1991, **55,** 566–568

[53] **van Genuchten M Th; Leij F J** On estimating the hydraulic properties of unsaturated soils. In Proceedings of the International Workshop, Indirect Methods for Estimating the Hydraulic Properties of Unsaturated Soils (van Genuchten M Th; Leij F J; Lund L J eds), Pp. 1–14. University of California, Riverside, 1992

[54] **van Genuchten M Th; Nielsen D R** On describing and predicting the hydraulic properties of unsaturated soils. Annales Geophysics, 1985, **3,** 615–628

[55] **Mualem Y** Hydraulic conductivity of unsaturated soils: Prediction and formulas. In: Methods of Soil Analysis, Part 1, Physical and Mineralogical Methods, 2nd edn (Klute A ed), Pp. 799–824. ASA and SSSA, Madison, WI, 1985

[56] **Nielsen D R; Luckner L** Theoretical aspects to estimate reasonable initial parameters and range limits in identification procedures for soil hydraulic properties. In: Proceedings of the International Workshop, Indirect Methods for Estimating the Hydraulic Properties of Unsaturated Soils, (van Genuchten M Th; Leij F J; Lund L J eds), Pp. 147–160. University of California, Riverside, 1992

[57] **Othmer H; Diekkrüger B; Kutilek M** Bimodal porosity and unsaturated hydraulic conductivity. Soil Science, 1991, **152,** 139–150

[58] **Ross P J; Smettem K R J** Describing soil hydraulic properties with sums of simple functions. Soil Science Society of America Journal, 1993, **57,** 26–29

[59] **Durner W** Hydraulic conductivity estimation for soils with heterogeneous pore structure. Water Resources Research, 1994, **30,** 211–223

[60] **Mallants D; Tseng P H; Toride N; Timmerman A; Feyen J** Evaluation of multimodal hydraulic functions in characterizing a heterogeneous field soil. Journal of Hydrology, 1997, **195,** 172–199

[61] **Gerke H H; van Genuchten M Th** A dual-porosity model for simulating the preferential movement of water and solutes in structured porous media. Water Resources Research, 1993, **29,** 305–319

[62] **Chen C; Wagenet R J** Simulation of water and chemicals in macropore soils Part 1: representation of the equivalent macropore influence and its effect on soilwater flow. Journal of Hydrology, 1992, **130,** 105–126

[63] **Chen C; Wagenet R J** Simulation of water and chemicals in macropore soils. Part 2: Application of linear filter theory. Journal of Hydrology, 1992, **130,** 127–149

[64] **Jarvis N J; Bergström L; Dik P E** Modelling water and solute transport in macroporous soil. II: chloride breakthrough under non-steady flow. Journal of Soil Science, 1991, **42,** 71–81

[65] **Jarvis N J; Jansson P E; Dik P E; Messing I** Modeling water and solute transport in macroporous soil. I. Model description and sensitivity analysis. Journal of Soil Science, 1991, **42,** 59–70

[66] **Gerke H H; van Genuchten M Th** Evaluation of a first-order water transfer term for variably saturated dual-porosity flow models. Water Resources Research, 1993, **29,** 1225–1238

[67] **van Genuchten M Th; Dalton F N** Models for simulating salt movement in aggregated field soils. Geoderma, 1986, **38,** 165–183

[68] **Saxena R K; Jarvis N J; Bergström L** Interpreting non-steady state tracer breakthrough experiments in sand and clay soils using a dual-porosity model. Journal of Hydrology, 1994, **162,** 279–298

[69] **Smith R E; Diekkrüger B** Effective soil water characteristics and ensemble soil water profiles in heterogeneous soils. Water Resources Research, 1996, **32,** 1993–2002

[70] **Rehfeldt K R; Boggs J M; Gelhar L W** Field study of dispersion in a heterogeneous aquifer, 3. Geostatistical analysis of hydraulic conductivity. Water Resources Research, 1992, **28,** 3309–3324

[71] **Cressie N A C** Statistics for Spatial Data, 900 Pp. New York: Wiley, 1993

[72] **Deutsch C V; Journal A G** GSLIB, Geostatistical Software Library and User's Guide, 340Pp. New York: Oxford University Press, 1992

[73] **Miller E E; Miller R D** Physical theory for capillary flow phenomena. Journal of Applied Physics, 1956, **27,** 324–332

[74] **Tillotson P M; Nielsen D R** Scale factors in soil science. Soil Science Society of America Journal, 1984, **48,** 953–959

[75] **Simmons C S; Nielsen D R; Biggar J W** Scaling of field-measured soil water properties. Hilgardia, 1979, **47,** 77–154

[76] **Vogel T; Cislerova M; Hopmans J W** Porous media with linearly variable hydraulic properties. Water Resources Research, 1991, **27,** 2735–2741

[77] **Warrick A W; Mullen G J; Nielsen D R** Scaling field-measured soil hydraulic properties using a similar media concept. Water Resources Research, 1977, **13,** 355–362

[78] **Hopmans J** A comparison of various methods to scale soil hydraulic properties. Journal of Hydrology, 1987, **93,** 241–256

[79] **Dagan G; Bresler E** Solute dispersion in unsaturated heterogeneous soil at field scale: I. Theory. Soil Science Society of America Journal, 1979, **43,** 461–467

[80] **Bresler E; Dagan G** Solute dispersion in unsaturated heterogeneous soil at field scale: II. Applications. Soil Science Society of America Journal, 1979, **43,** 467–472

[81] **Khan A U H; Jury W A** A laboratory study of the dispersion scale effect in column outflow experiments. Journal of Contaminant Hydrology, 1990, **5,** 119–131

[82] **Vanclooster M; Mallants D; Vanderborght J; Diels J; Van Orshoven J; Feyen J** Monitoring solute transport in a multi-layered sandy lysimeter using time domain reflectometry. Soil Science Society of America Journal, 1995, **59,** 337–344

[83] **Ellsworth T R; Shouse P J; Skaggs T H; Jobes J A; Fargerlund J** Solute transport in unsaturated soil: Experimental design, parameter estimation, and model discrimination. Soil Science Society of America Journal, 1996, **60,** 397–407

[84] **Toride N; Leij F J** Convective–dispersive stream tube model for field-scale solute transport: I. Moment analysis. Soil Science Society of America Journal, 1996, **60,** 342–352

[85] **Toride N; Leij F J** Convective–dispersive stream tube model for field-scale solute transport: II. Examples and calibration. Soil Science Society of America Journal, 1996, **60,** 352–461

[86] **Destouni G** Stochastic modelling of solute flux in the unsaturated zone at the field scale. Journal of Hydrology, 1993, **143,** 45–61

[87] **Yeh T C J** Stochastic modelling of groundwater flow and solute transport in aquifers. Hydrological Processes, 1992, **6,** 369–395

[88] **Mantoglou A; Wilson J L** The turning bands method for simulation of random fields using line generation by a spectral method. Water Resources Research, 1982, **18,** 1379–1394

[89] **Robin M J L; Gutjahr A L; Sudicky E A; Wilson J L** Cross-correlated random field generation with the direct Fourier transform method. Water Resources Research, 1993, **29,** 2385–2397

90 **Šimůnek J; Vogel T; van Genuchten M Th** The SWMS_2D code for simulating water flow and solute transport in two-dimensional variably saturated media. Research Report No. 132, U.S. Salinity Lab., ARS, USDA, Riverside, CA, USA, 1994

91 **Tompkins J A; Gan K C; Wheater H S; Hirano F** Prediction of solute dispersion in heterogeneous porous media: effects of ergodicity and hydraulic conductivity discretisation. Journal of Hydrology, 1994, **159,** 105–123

92 **Rubin Y** Stochastic modeling of macrodispersion in heterogeneous porous media. Water Resources Research, 1990, **26,** 133–141

93 **Kinzelbach W; Uffink G** The random walk method and extensions in groundwater modeling. In Transport Processes in Porous Media, edited by (Bear J; Corapciolu M Y, eds), Pp. 761–787. USA; Kluwer Academic, Norwell, MA. 1991

94 **Kitanidis P K** Particle-tracking equations for the solution of the convection-dispersion equation with variable coefficients. Water Resources Research, 1994, **30,** 3225–3227

95 **Huyakorn P S; Pinder G F** Computational Methods in Subsurface Flow. Academic Press, London United Kingdom, 1983

96 **Perrochet P; Bérod D** Stability of the standard Crank–Nicolson–Galerkin scheme applied to the diffusion–convection equation: some new insights. Water Resources Research, 1993, **29,** 3291–3297

97 **Russo D** Stochastic modeling of solute flux in a heterogeneous partially saturated porous formation. Water Resources Research, 1993, **29,** 1731–1744

98 **Roth K** Steady state flow in an unsaturated, two-dimensional macroscopically homogeneous. Miller-similar medium. Water Resources Research, 1995, **31,** 2121–2140

99 **Harther T; Yeh T -C** Stochastic analysis of solute transport in heterogeneous, variably saturated soils. Water Resources Research, 1996, **32,** 1585–1595

100 **Rockhold M L; Rossi R E; Hills R G** Application of similar media scaling and conditional simulation for modeling water flow and tritium transport at the Las Cruces Trench Site. Water Resources Research, 1996, **32,** 595–609

101 **Wierenga P J; Hills R G; Hudson D B** The Las Cruces Trench Site: Characterization, experimental results, and one-dimensional flow predictions. Water Resources Research, 1991, **27,** 2695–2705

102 **Bakr A A; Gelhar L W; Gutjahr A L; MacMillan J R** Stochastic analysis of spatial variability in subsurface flows. 1. Comparison of one and three-dimensional flows. Water Resources Research, 1978, **14,** 263–271

103 **Gutjahr A L; Gelhar L W; Bakr A A; MacMillan J R** Stochastic analysis of spatial variability in subsurface flows. 2. Evaluation and application. Water Resources Research, 1978, **14,** 953–959

104 **Yeh T C J; Gelhar L W; Gutjahr A L** Stochastic analysis of unsaturated flow in heterogeneous soils. 1. Statistically isotropic media. Water Resources Research, 1985, **21,** 447–456

105 **Yeh T C J; Gelhar L W; Gutjahr A L** Stochastic analysis of unsaturated flow in heterogeneous soils. 2. Statistically anisotropic media with variable *a*. Water Resources Research, 1985, **21,** 457–464

106 **Mantoglou A; Gelhar L W** Stochastic modeling of large-scale transient unsaturated flow systems. Water Resources Research, 1987, **23,** 37–46

107 **Mantoglou A; Gelhar L W** Capillary tension head variance, mean soil moisture content, and effective specific soil moisture capacity of transient unsaturated flow in stratified soils. Water Resources Research, 1987, **23,** 47–56

108 **Mantoglou A; Gelhar L W** Effective hydraulic conductivities of transient unsaturated flow in stratified soils. Water Resources Research, 1987, **23,** 57–67

109 **Polmann D J; McLaughlin D; Luis S; Gelhar L W; Ababou R** Stochastic modeling of large-scale flow in heterogeneous unsaturated soils. Water Resources Research, 1991, **27,** 1447–1458

110 **Jensen K H; Mantoglou A** Application of stochastic unsaturated flow theory, numerical simulations, and comparison to field observations. Water Resources Research, 1992, **28,** 269–284

111 **Gelhar L W; Axness C L** Three-dimensional stochastic analysis of macrodispersion in aquifers. Water Resources Research, 1983, **19,** 161–180

112 **Naff R L** On the nature of the dispersive flux in saturated heterogeneous porous media. Water Resources Research, 1990, **26,** 1013–1026

113 **Russo D** Stochastic modeling of macrodispersion for solute transport in a heterogeneous unsaturated porous formation. Water Resources Research, 1993, **29,** 383–397

114 **Shapiro A M; Cvetkovic V D** Stochastic analysis of solute arrival time in heterogeneous porous media. Water Resources Research, 1988, **24,** 1711–1718

115 **Dagan G; Cvetkovic C D; Shapiro A** A solute flux approach to transport in heterogeneous formations. 1. The general framework. Water Resources Research, 1992, **28,** 1369–1376

116 **Cvetkovic V D; Shapiro A; Dagan G** A solute flux approach to transport in heterogeneous formations. 2. Uncertainty analysis. Water Resources Research, 1992, **28,** 1377–1388

117 **Russo D** On the velocity covariance and transport modeling in heterogeneous anisotropic porous formations. 2. Unsaturated flow. Water Resources Research, 1995, **31,** 139–145

118 **Mohanty B P; Horton R; Ankeny M D** Infiltration and macroporosity under a row crop agricultural field in a glacial till soil. Soil Science, 1996, **161,** 205–213